UNIVERSITAT POLITÈCNICA DE VALÈNCIA

Escuela Técnica Superior de Ingeniería del Diseño

UNIVERSITAT POLITÈCNICA DE VALÈNCIA

School of Design Engineering

Fuel cell - powered adaptation of a light helicopter design and environmental impact analysis

End of Degree Project

Bachelor's Degree in Aerospace Engineering

AUTHOR: Morales López, Jesús

Tutor: Tiseira Izaguirre, Andrés Omar

Cotutor: López Juárez, Marcos

ACADEMIC YEAR: 2021/2022

Acknowledgements

The work that has been carried out with this project is dedicated to everybody that has helped me during my years as a student. To every teacher that has ever dedicated a moment to stop and solve the question I posed, specially this project's tutors, Andrés and Marcos, to whom I owe the success of my work. To the friends that accompanied me every step of the way for the last four years. To my wonderful girlfriend Paula, without whom I cannot imagine any second of my past and my future. To my family, the most generous and caring group of people I will ever meet. Specially to my parents, Mila and Jesús, and my sweet sister, Marta, I am so lucky to have you with me in this beautiful ride.

Thank you.

Abstract

Using the increasingly popular and evergrowing technology of hydrogen based fuel cells, given their environmental advantages over fossil fuels, and starting from a previously calculated, statistically-based design of a light helicopter for civil use, the aircraft has been recalculated including the new power system, iteratively dimensioned and optimized for different applications: from urban and inter-urban commutes to unmanned operations.

This iterative methodology was carried out obtaining approximations of cruise and ascending/descending power, as well as the fuel required to complete the mission accounting for the current state of the art of the involved technology. In the development of the adapted version, focus was centered on the new power system, including careful considerations about the performance of its components by using dynamic simulations of the fuel cell system based on air usage optimization as well as considering the aerodynamic effect of exterior hydrogen tanks. Additionally, future design considerations were suggested based on the work of previous authors involving aerodynamics, materials and space distribution in order to both maximize the potential and leave room for the next steps in terms of improvement through more specific studies.

To conclude, a life-cycle assessment (L.C.A.) was performed, studying the environmental impact of the designs compared to their predecessor and use the opportunity to discuss the current state of hydrogen production, as well as future challenges related with this technology.

Key words

fuel cell, hydrogen, light helicopter, life cycle assessment, UAV

Contents

List of Figures

List of Tables

Nomenclature

Latin symbols

a	Speed of sound	$[m/s]$
a_t	Profile lift curve slope	$[rad^{-1}]$
B	Tip loss coefficient	[-]
b	Number of rotor blades	[-]
c	Chord	$[m]$
C_T	Thrust coefficient	[-]
C_W	Weight coefficient	[-]
C_d	Profile drag coefficient	[-]
D	Drag	$[N]$
f	Equivalent flat plat surface	$[m^2]$
J	Polar moment of inertia	$[kg \cdot m^2]$
k	Surface rugosity	$[m]$
L	Length	$[m]$
L	Lift	$[N]$
M	Mach number	[-]
m	Mass	$[kg]$
p	Pressure	$[Pa]$, $[atm]$
R	Rotor radius	$[m]$
S	Surface	$[m^2]$
T	Thrust / Traction	$[N]$
V	Velocity	$[m/s]$

V	Volume	$[m^3]$
W	Weight	$[N]$

Greek symbols

δ_i	Parabolic polar parameters	[-], $[rad^{-1}]$, $[rad^{-2}]$
η	Efficiency	[-]
κ	Compressibility effects coefficient	[-]
λ	Inflow ratio	[-]
μ	Advance ratio	[-]
Ω	Blade angular velocity	$[rad^{-1}]$, $[rpm]$
ρ	Density	$[kg/m^3]$
σ	Solidity	[-]

Acronyms

$CAGR$	Compound annual growth rate	[-]
EEA	European Environment Agency	
$eVTOL$	Electric Vertical Takeoff and Landing aircraft	
FCV	Fuel Cell Vehicle	
FM	Figure of merit	[-]
GHG	Greenhouse Gases	
IEA	International Energy Agency	
LCA	Life Cycle Assesment	
LEZ	Low Emission Zone	
LHV	Lower Heating Value	[kWh/kg], [kWh/m^3]
$MTOW$	Maximum Takeoff Weight	[kg]
NP	Nominal Power	[kW]
$PM_{2.5}$	Particulate matter (under 2.5 microns)	
SAR	Search and Rescue	
UAM	Urban Air Mobility	
UAV	Unmanned Aerial Vehicle	

Subscripts

0	Parasitic
∞	Undisturbed flow
b	Rotor blades
DC	DC-DC converted
$eMotor$	Electric motor
f	Fuselage
FC	Fuel cell
FS	Fuel Storage
H	Helicopter
h	Rotor hub
i	Induced
mr	Main rotor
n	Iteration number
PD	Power devices
PL	Payload
ref	Reference
tr	Tail rotor
z	Ascending / Vertical

Chapter 1

Introduction

1.1 Historical background

The helicopter is undoubtedly one of the greatest technological achievements in the aeronautics field. The history of its success is one full of challenges that pushed the limits of our science.

The dream of flight, popularly accepted to be first accomplished by the Wright brothers in 1903, was achieved with a primitive but ingenious airplane model. By that time, the basis of fixed-wing aerodynamics had been settled and the field was experiencing a huge growth due to, at least in part, the increasing success of these flying machines. As the industry developed and the *Wright flyer* transitioned into the titans of the air we observe today, the limitations of fixed-wing aircraft were very much clear: airplanes needed to be continuously moving to fly.

Curiously, the very first attempts at flight did not suffer from this limitation. Indeed, the most ancient solution to the flight challenge consisted in rotorcraft: vehicles whose lifting force was generated by a rotatory wing. This idea can be first found in the Chinese "tops" [34], simple toys composed of feathers perpendicularly placed at the end of a stick which, inspired by the fight of sycamore and maple tree seeds, would sustain themselves in the air by auto-rotation.

Conceptual models for rotorcraft began to be developed in the Renaissance by the hands of no other than Leonardo DaVinci. His sketches for the "aerial screw" date back to 1483 and describe that the helical mechanism should be "rotated with speed such that the screw bores through the air and climbs high enough". While his design was never tested, small models based on this rotation were developed in the 18^{th} century: Lomonosov (1754) and Launoy (1783) developed mechanically powered versions of the "tops", while Paucton (1768) proposed one of the first concepts of a human carrying helicopter in his scientific paper *Théorie de la vis D'Archimède* [33]. Even greater contributions came from the hand of Sir George Cayley in the beginning of the 19^{th} century, including documents laying down the scientific principles of aerodynamics and several rotorcraft conceptual models which, for the time, provided incredible insight into the complexity of the project.

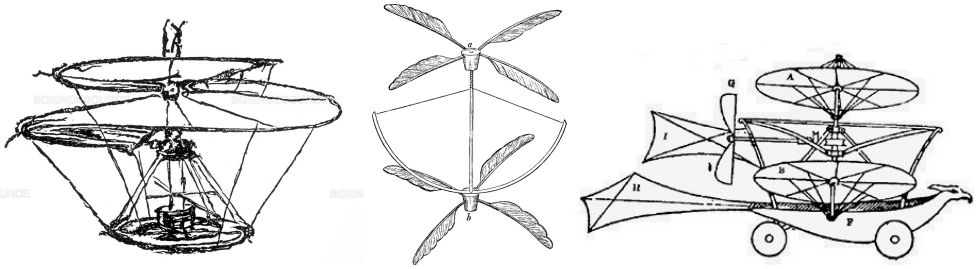

Figure 1.1: Different conceptual models for helicopters developed throughout history. From left to right, DaVinci's "aerial screw" (1483), Lomonosov's "top" (1754) and Cayley's "aerial carriage" (1843).

Attempts at building these devices continued to be carried out in the 1870s and 1880s, where it is interesting to outline the experiments carried out by Thomas Edison [34], whose scientific approach helped to point out the main challenges for the development of these machines, and which to this day continue to be relevant to describe the topic. Mainly, during this time there was a lack of aerodynamic understanding of vertical flight in comparison to forward flight, which extended to the problem of counteracting the torque-reaction without further increasing the mechanical complexity. Additionally, it was demonstrated that steam engines just did not fit this application, as higher power to weight ratios were needed (and internal combustion engines would not be developed until the 1920s). Developments continued to be made, partially powered by the achievements of fixed-wing aviation, and with those developments, new challenged arrived: need for weight reduction, vibration and control problems, etc.

Modern-day helicopters are refined and sophisticated pieces of technology, product of more than a century of intensive research and development. On the way to their full realization, incredible insight in the fields of aerodynamics, materials, vibrations and propulsion were obtained. Though extremely complex, their benefits clearly outweighed the problems encountered, as they possess characteristics that are not attainable by any other aircraft. The technological void left in the low speed region of the flight domain of fixed-wing aircraft could now be filled with these devices. Even compared to other rotorcraft, the helicopters are superior: they are lighter, can hover more efficiently and provide a higher traction to power ratio than any of their counterparts. Modern designs are also very flexible, which have made them suitable for countless applications: transport, search and rescue operations, surveillance or homeland defense, only to name a few.

The increasingly rapid development of the aerospace sector has also been reflected on the helicopter segment, and for good reason. Their unique operational advantages against conventional fixed-wing aircraft have cleared the way to a new world of concepts only achievable through these *ungainly, aerodynamic mavericks* [7].

1.2 Motivation and state of the art

After slightly less than a century of helicopter flight, technological developments are opening the doors of new market segments. Studies are currently projecting a CAGR of 4% for the decade [11], [26] as the land-based transportation system is reaching its maximum density in some parts of the world.

The use of light helicopters particularly has seen an exceptional increase in demand in the sectors of surveillance, emergency aid and, more interestingly, urban mobility. As the cities grow taller, more opportunities have emerged for light helicopters to appear as a solution for both traffic congestion and air pollution, since their reduced weight allow them to be operated with electric motors. In fact, companies such as *Joby Aviation* (U.S.A.) and *Ola cabs* (India) have launched programs (*Uber Elevate* and *Ola air*, respectively) aiming to supply the helicopter cab hailing market in cities where traffic congestion is at an all time high [18], [37].

Their potential environmental benefits are also raising interest given the current actions taking place in cities around the world aiming at improving the air quality, as well as their liveability and safety. Current studies show that the commuting system represents approximately 25% of the total CO_2 emissions in Europe. It is well known that a high level of air pollution has an immediate burden on the health of the inhabitants: increased risk of cancer, ischaemic heart disease, chronic obstructive pulmonary disease or neurological conditions are among the most frequent consequences of a poor air quality. Recent EEA reports found an estimated 13% of the total deaths in Europe to have been caused by environmental conditions, being these numbers specially worrisome in Eastern Europe. *Figure 1.2* reflects the clear correlation between the mean concentration of $PM_{2,5}$ and the percentage of deaths attributed to the environment, a measure that not only accounts for air quality, but also noise pollution, extreme weather conditions, chemicals, etc.

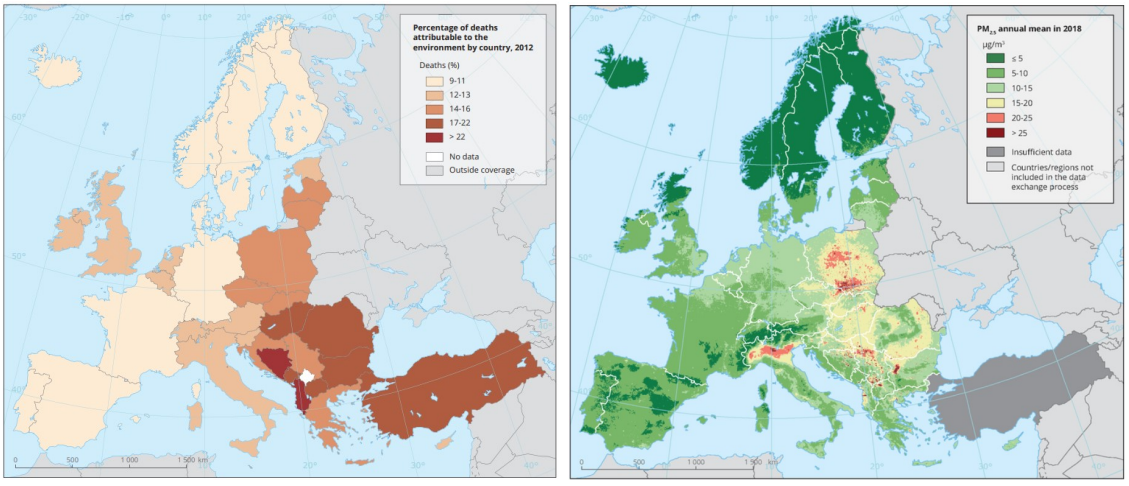

Figure 1.2: Correlation between areas in Europe with high concentrations of PM2,5 and the percentage of deaths attributed to the environment. Source: EEA [24].

In the light of these studies, countries have begun to question the current mobility system, implementing palliative measures such as the creation of more than 250 low emission zones (LEZs) in European urban nuclei, financial support to foment the purchase of electric cars or investments in infrastructure dedicated to the use of bicycles. While merit

has to be attributed to these initiatives, some are yet to be proven beneficial such as LEZs and the others do not address the traffic congestion dilemma at all.

All of these factors are bringing a perfect storm in which urban mobility is suffering a steady transformation where aerial vehicles could find a new market niche. In this sense, the *Clean Sky 2* [9] initiative frames the present environmental challenges and their proposed actions for aircraft manufacturers and operators to undertake, in hopes of reducing our industry's footprint on climate change.

Among one of this initiative's talking points, fuel cells appear as a promising solution to electrify parts of the aircraft, on-ground units and more. The most popular variant of a fuel cell is one where hydrogen acting as a fuel, and oxygen as the oxydizer, generates electricity by mean of a redox chemical reaction where the byproduct is simply water. Technology around this concept has been consistently flooding with developments in the last two decades, as more powerful and compact fuel cells are being developed. This fact, combined with the price increase in fossil fuels and the progress in the hydrogen generation field, are causing a rapid advancement towards the so-called "hydrogen economy", and while still having well-known issues such as indirect pollution, transport and storage, it only seems inevitable that hydrogen will slowly become the protagonist of the new age of fuels. Indeed, the International Energy Agency (IEA) predictions locate the rise of hydrogen vehicles for the next decade as a fairly safe bet, going as far as expecting a 20% of the total market share for FCV in 2050 [57].

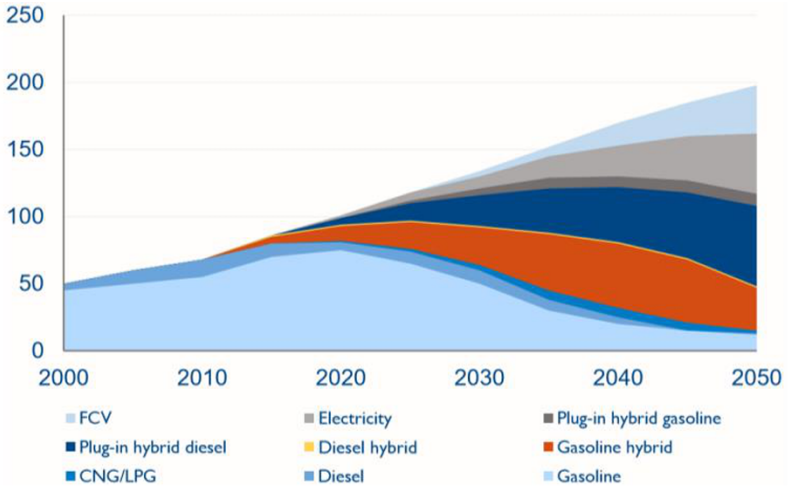

Figure 1.3: Projected vehicles sales volume by fuel type. Source: IEA [57].

While many applications are suitable for hydrogen as a fuel, aerial vehicles are clearly benefited by its high specific power, fuel cell safe operation and reliability. The feasibility of a light helicopter powered by a hydrogen fuel cell has been already studied by several authors and current technology allows for it to be at least conceptually viable [15]. Still, many aspects of their operation are yet to be studied: dimensioning, location of the hydrogen tanks and development of appropriate propulsive units among some of them, which this project is precisely centered around.

1.3 Objectives and structure of the project

The previous set of ideas summarize the motivation behind this project, where the main objective will be to contribute to the current development of light helicopters and their design, aiming to focus on their urban mobility potential and environmental sustainability.

In order to do so, a previously developed conceptual model of a light helicopter will be used as a reference and adapted to be powered by a hydrogen fuel cell and operable for both tripulated commutes and unmanned missions. To complete this goal, the following points will be developed, following an iterative process:

- Dimensioning of the new propulsive plant and power system of the helicopter.
- Analysis of different alternatives for hydrogen storage systems and their location on the aircraft.
- Aerodynamic optimization of the design through the helicopter actuations.

After obtaining the conceptual result, aspects related to the potential future model will be studied, considering not only aerodynamics, but also mechanical, constructive and economical factors into the matter.

Finally, a comprehensive *Life-Cycle Assessment* (LCA) will be performed in order to study the environmental impact of the new design and compare it to its predecessor, with the objective of demystifying hydrogen technology and assess whether or not is the technology ready to start carrying the hopes to reduce the carbon footprint of aviation.

The project will follow a structure based on different chapters, covering the different aspects to be addressed. First, a deeper analysis of the market opportunities for light helicopters will be exposed, followed by the theoretical basis of the study, mainly the aerodynamic design of helicopters and the principles of hydrogen-powered propulsion. After explaining in more detail the iterative process followed, the results will be exposed and analyzed, as they lead into a set of reflections on the challenges still to be faced. The LCA will be then developed, introducing its considerations and structure, and followed by the results of the study. Finally, a summary of the main conclusions of the project will be presented with the objective of closing the paper with a check on the initial goals and take-aways.

Chapter 2

Light helicopter market overview

The current helicopter services market size is located around $30 billion, having an estimate of 20% of the total share currently dedicated to light helicopters. Most market consultants agree that future looks bright for the helicopter industry, expecting a CAGR between 4%-6%. Many factors are driving the light helicopter market to a more beneficial position, so it is worth taking a closer look at the arguments to evaluate if the optimism is founded.

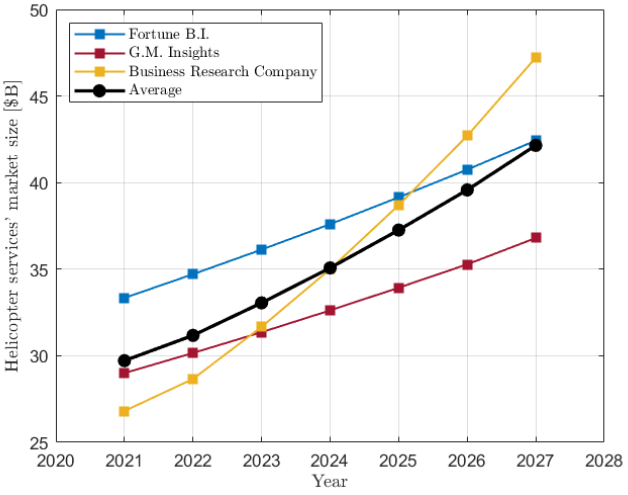

Figure 2.1: Forecast of the temporal evolution of the helicopter services market according to several consultant companies. Sources: Fortune Business Insights [26], G.M. Insights [25] and Business Research Company [10].

Formally speaking, a light helicopter is generally accepted to have a maximum gross weight of 4,000 kg, even if there isn't a proper established classification. These aircraft have been historically popular for recreational use, having for instance the Cicaré-CH7, the Dynali H2s or the RotorWay A600 as premier examples of this application. However, light helicopters have also grown because of their extreme design versatility, allowing for a very diverse range of applications, for example:

- **Agricultural**: Aircraft have always found their use in agriculture, specially for crop spraying. This task, which originally used small-sized planes to release the products on the field has been taken over by light helicopters given their lower takeoff requirements, enhanced precision and better performance in smaller, irregular fields and areas surrounded with obstacles such as trees or power lines. They also hold numerous other lesser known applications in this industry such as preventing frost damage or removing rain in low altitude flights. Helicopters such as the Bell 206 or, more recently, the UAV Align Demeter E1 are key examples.
- **Search and rescue (S.A.R.)**: Light helicopters are being posed as a clear candidate to replace ordinary helicopter models used for law enforcement due to their logistical advantages in terms of maneuvering, storage and transportation. While admittedly, their use is limited by the reduced payload they are able to hold in comparison to other models, they are becoming more and more popular for surveillance applications, being the MD 500E the most popular example used in public safety missions.
- **Medical emergency transport**: Given their unique characteristics, light helicopters have found a market niche in the field of medical transport, having this need emphasized during the COVID-19 pandemic. Examples such as the AS350 or the EC130 are references in this field given their lower operation costs, mission flexibility and ease of cabin customization.

These applications are expected to continue to have a large impact in the years to come, specially in countries such as India or China with the rise of the *smart city* projects. Private medical and surveillance services are expected to continue funding light helicopter development for future projects as the technology reaches sustainable operating costs.

In more recent times, however, a new exciting application has made itself available for the helicopter industry, suiting specially light helicopters and that is in fact urban mobility. Economic development has led to an unprecedented increase in urban population density and has allowed the inhabitants of cities to afford privately owned vehicles. It has been estimated that 50 % of European workers use privately-owned vehicles daily for their commutes, while only 16 % use public transport [21], a statistic that has been further affected by the health crisis suffered in the last couple of years.

With cities becoming more populated and congested, more concerns about the current mobility system have been raised. On average, an European citizen that has worked at the same place during the last 20 years has seen the time to reach that workplace increase by 10% and up to 20% depending on the country of origin as findings by Giménez-Nadal, Molina and Velilla [21] show that commuting times follow similar increasing patterns in all of the different regions in Europe.

The increase in commute time has had both health and economic effects on civilians. In fact, from a purely economic point of view, it has been estimated that highly dense metropolitan areas such as Manhattan experience annual losses of approximately $20 billion due excess fuel burning [43]. Adding up the proven health impact, mainly due to stress and air pollution, to the economical and environmental burden, traffic congestion has quickly become one of the main immediate challenges of urban development in this generation.

Helicopters have appeared in the discussion as the obvious beneficiary, since it is clear that modes of transportation beyond traditional ground-based vehicles need to be explored. Around the world, several logistics companies and aviation agencies ventured into urban air mobility by means of flying taxi services.

More specifically, light helicopters, which offer an already proven versatility, also fit within environmental guidelines since their architecture allows for the introduction of fully electric power systems that offer an energy efficient, safer and quieter commute than any other helicopter to date. The most immediate example is *Uber Elevate*, set to launch on 2023 after different setbacks in the last two years, but other companies both experienced in the aircraft sector such as Zephyr Airworks or Airbus (with the Cora and Vahana prototypes respectively) and new to the game such as Toyota or Hyundai are funding ambitious projects to be the first eVTOL taxi operators.

Figure 2.2: Current advanced prototypes for air taxis in the form of eVTOL by Airbus (left) and Zephyr Airworks (right).

Success stories are occurring across the industry: in the United States alone, studies suggest that the top 10 startups have raised approximately $6 billion in funding [66], Toyota has recently invested $394 million in Joby Aviation [38], Hyandai's creation of the *Supernal* air taxi division has successfully collaborated with *Urban-Air Port* to develop the necessary infrastructure for UAM projects [8] and even governmental agreements have occurred in the case of Zephyr Airworks with New Zealand [65]. In total, the air taxi market represents, according to Allied Market Research [3], around $800 million, specially centered in America.

The market is clearly shifting and, while still in development, the take-off of air taxis seems inevitable. Future estimates range wildly, from $6 billion in 2030 [3] to others speculating with $4 trillion by 2040 [50], but all coincide that a minimum of 25 % CAGR is expected for the following decade.

Combining the different market segments, it is clear that the expected growth in the light helicopter industry is founded, even raising its potential to be absolutely game-changing for the industry if UAM plans continue their current trend, and understanding the value behind this technology is one of the main motivations for this study.

Chapter 3

Theoretical background

After expanding on the motivation of the study, the objective for the following chapter is to present a comprehensive theoretical background to the concepts developed in the project: mainly the aerodynamic analysis of helicopters and the working principles of fuel cells.

Given that these fields are extremely deep and complex, only the main useful concepts will be developed. In the case of the aerodynamic analysis, focus will be centered around the power calculation of conceptual rotors, correction models that may be applied as well as rotor actuations. For fuel cells, a descriptive analysis of their working principle and architecture will be introduced, leaving some room to discuss their advantages, weaknesses and current challenges.

3.1 Helicopter aerodynamic analysis

The methodology used for first level estimations of power consumption of a rotor involves mainly two models: momentum conservation theory and blade element analysis. Furthermore, their combination leads to efficient calculation mechanisms with relatively high accuracy and it is the basis for this study.

3.1.1 Momentum theory analysis

Momentum theory is the most widespread method to obtain a first approximation of the rotor performance, given its simplicity yet relatively precise results. It is based on the application of integral conservation equations to a simplified airflow field.

In order to better understand the fundamentals, it is helpful to describe the airflow state around a hovering rotor. This situation, with null vertical and horizontal speeds for the helicopter, is the simplest case for helicopter aerodynamics since the flow field is azimuthially axisymmetric. Empirical observations of the airflow state under these conditions lead to the main simplifying assumptions of the momentum theory model:

- The rotor can be represented as an infinitesimally thin "actuator disk" over which a pressure difference exists.
- The fluid velocity is uniformly increased as it travels through the rotor, so there is no jump in velocity across the disk
- The thrust vector results from the finite jump in pressure accross the rotor.
- There seems to be a "wake boundary" or "slipstream" past which velocity can be expected negligible compared to the inside.
- The diameter of the slipstream is reduced accross the rotor, accounting for the increase of the slipstream velocity.

With these simplifications, the fluid domain around a rotor can be generally characterized in a clear and efficient manner. *Figure 3.1* is the most common way to reflect this fluid domain according to Momentum Theory: thrust (T) is a force vector perpendicular to the rotor surface created by the pressure gradient between both sides of the rotor, and as power is transmitted to the rotor shaft in the form of torque, the work done on the rotor transmits kinetic energy to the slipstream causing an increase in velocity below the disk by an amount denominated "induced velocity", which can be though of as an unavoidable power loss required to generate thrust.

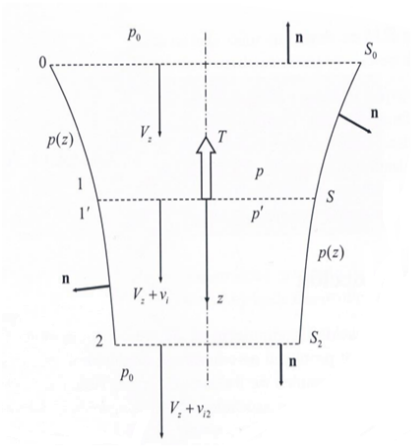

Figure 3.1: Fluid domain described in Momentum Theory. Source: Cuerva et al. [13]

From this point, it is relatively trivial to apply conservation equations for mass, momentum and energy to obtain analytical expressions for the unknowns in the system.

For forward flight, the analysis gets more complicated since by definition, helicopters will need to tilt the rotor plane forward in order to both sustain the weight of the aircraft and propel it in the desired direction.

Once the model is set up, shown in *Figure 3.2*, a similar procedure can be applied, obtaining a slightly more complex calculation method though still being very efficient compared to the complexity of the real system. In the traditional development of this theory, formally generalized by Hermann Glauert, it is even acknowledged that some of the decisions taken (for instance, the calculation of the resultant velocity across the disk) have no other rigor than to reduce the theory back to the regular hovering results under

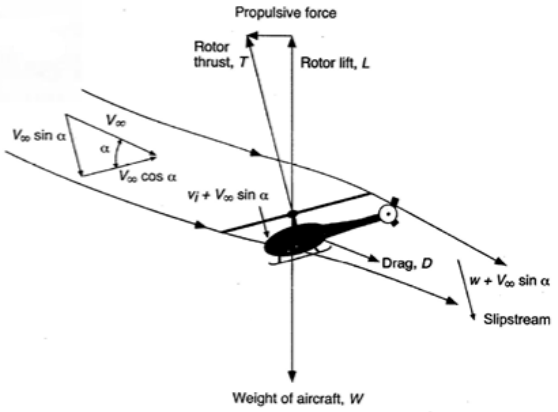

Figure 3.2: Fluid domain described by Momentum Theory in forward flight. Note that angles are exaggerated for clarity. Source: Leishman [33].

null forward speed. Given the strong hypothesis applied, additional corrections will be needed, as they will be introduced later on.

3.1.2 Blade element analysis

In contrast to momentum theory, the blade element analysis is based around the assuption that each blade section can be calculated as a generic aerodynamic profile generating its own forces and moments. Compared to their fixed-wing counterparts, however, flow across the blade is not uniform given its rotatory nature, so this factor is accounted through a modification of the angle of attack of each blade element.

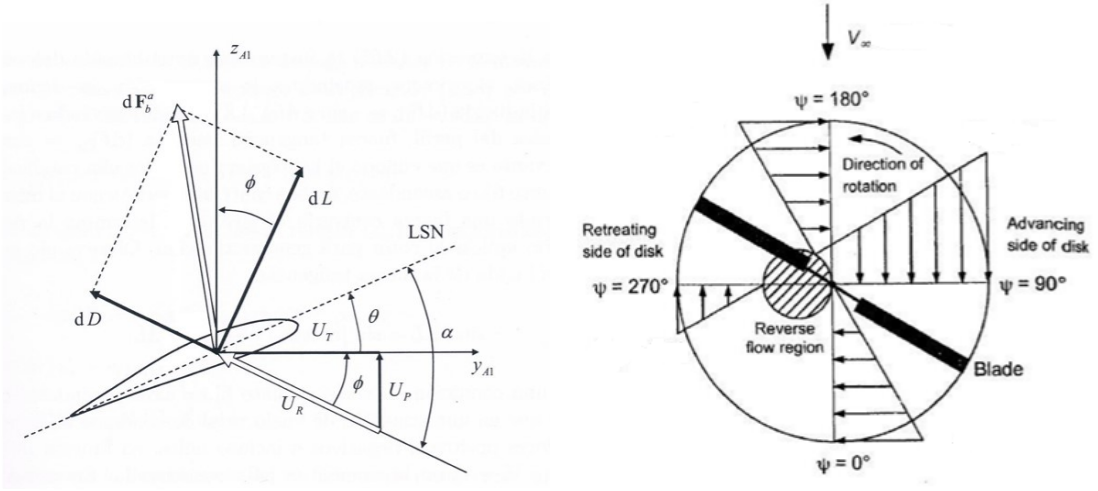

Figure 3.3: Blade element theory analyzes the rotor disk as individual infinite two-dimensional profiles (left) to account for the radial and azimuthal distribution of aerodynamic parameters on the disk like velocity (right). Source: Leishman [33].

This theory, mainly attributed to Drzewiecki and Lanchester, forms the basis of modern rotor aerodynamics since it provides an approximation to the radial and azimuthal

distributions of the aerodynamic parameters over the rotor. It allows to introduce aerodynamic performance data for the profile such as the lift and drag coefficients and rapidly obtain a more complex representation of the flow, being additionally very easy to combine with the momentum theory. The integration of the calculated distributions result in a theoretically more accurate result for the torque, power and ultimately, thrust generated by the system.

It has important drawbacks, however, since the two-dimensional profile approximation yields poor results without additional corrections coming from more complex aerodynamic models. Note for example how, as it can be seen in *Figure 3.3*, in forward flight there is a region where the blade elements experience a velocity entering from the trailing edge (the so called "inverse flow region"). The analysis of this area cannot be covered using the regular blade element theory and semi-empirical corrections must be used.

3.1.3 Combination of the models and common corrections

The two previous theories have advantages and drawbacks but, as first proposed by Gustafson and Gessow, they are extermely compatible. The resulting method is a hybrid based around the assumption that the parameters calculated in each theory, if correct, should be the same.

With this idea in mind, the original control volume in momentum theory becomes an annulus of differential width located at some distance from the shaft axis with a similar contraction below the rotor so that it is possible to apply both conservation equations and blade element analysis procedures, liberating this last method from its limiting two-dimensional hypothesis.

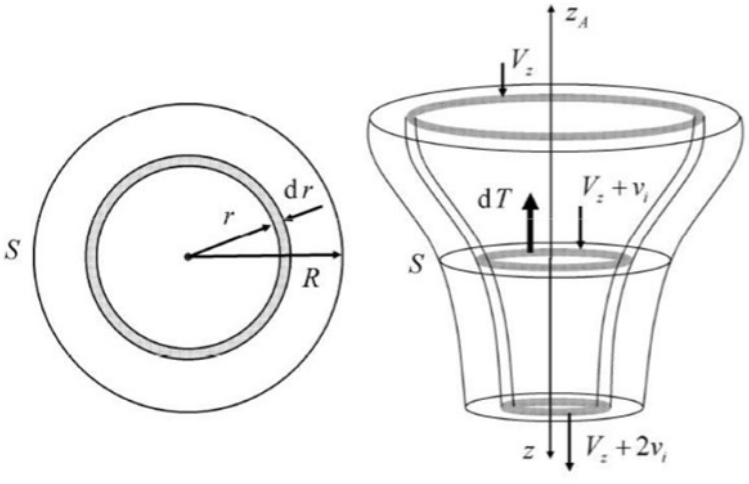

Figure 3.4: Annulus control volume used to apply momentum theory under a blade element analysis scope. Source: Cuerva et al. [13]

The combination of these theories naturally reduces to a method to calculate radial distributions of induced velocity across the rotor, which in turn results useful to calculate the rest of parameters. The value behind this method, however, is the obtained qualitative characteristics of the flow which lead to both conclusions about the optimal rotor and blade

architecture and limitating factors. The methods also results in important corrections applicable to obtain a more accurate estimation of rotor power.

Some of the most relevant correction models account for:

- **Non-ideal effects:** Momentum theory by itself does not account for viscous effects, while blade element analysis introduces them from a two-dimensional profile point of view. A better correction can be obtained also introducing additional terms that account for the drag generated by the structure and reverse flow effects (see *Figure 3.3*).
- **Tip loss:** It can be experimentally observed that as the blades rotate, they leave a trail of vortexes at the tips that increase the local inflow and effectively reduce the lifting capability. The phenomenon is more commonly represented by a tip-loss factor B representing a reduction of the effective blade radius and can be found to be between 0.95-0.98 for most rotors. Alternative and more complex models exist, such as Prandtl's function, but will not be used during the project.
- **Compressibility corrections and tip relief:** When introducing the model's aerodynamic parameters such as the lift curve slope, it is typically done assuming independence of Mach number for simplicity, which is known to be untrue in the case of elevated Mach numbers such as at the blade tips. However, these effects have been experimentally proven to not be relevant until the profile drag divergence Mach number is well exceeded, so the so-called "tip relief" effects add an additional layer of corrections. In general, compressibility effects in forward flight usually account for an additionally 10-15% of the calculated theoretical result.

3.1.4 Helicopter performance and actuations

After applying the aforementioned models, a good estimation of the rotor necessary power output can be estimated. This value is usually divided in serveral terms: induced power (amount transmitted to the fluid in order to carry out the maneuver according to momentum theory), profile power (required to overcome viscous losses at the blades and due to reverse flow) and parasitic power (required to overcome viscous losses of the remaining elements of the helicopter as it moves through the fluid).

The total power required can be then represented, often adimensionalized with respect to hovering results for convenience, as a function of helicopter velocity, resulting in what is commonly know as the power-curve of the helicopter.

$$\frac{P_{mr}}{P_{i0}} = \kappa \frac{v_i}{v_{i0}} + \frac{V_z}{v_{i0}} + \frac{f}{4S}\left(\frac{V_f}{v_{i0}}\right)^3 + \frac{\sigma \cdot C_{d0}}{16\left(\frac{v_{i0}}{\Omega R}\right)^3}\left[1 + K\left(\frac{V_H}{v_{i0}}\right)^2 \frac{C_w}{2}\right] \tag{3.1}$$

Note that the different components of the required power are represented in the equation: from left to right, induced power, power required to ascend, fuselage parasitic power and profile parasitic power. Under the consideration that the induced velocity is much smaller than helicopter forward speed ($v_i << V_H$), the equation can be reduced to what is commonly known as the "high speed approximation", shown in *Equation 3.2*.

$$\frac{P_{mr}}{P_{i0}} = \kappa \frac{v_{i0}}{V_H} + \frac{f}{4S}\left(\frac{V_H}{v_{i0}}\right)^3 + \frac{\sigma \cdot C_{d0}}{16\left(\frac{v_{i0}}{\Omega R}\right)^3}\left[1 + K\left(\frac{V_H}{v_{i0}}\right)^2 \frac{C_w}{2}\right] \tag{3.2}$$

The generic shape generated by this equation is shown in *Figure 3.5*. From this result, several conclusions can be drawn:

- The main source of power consumption comes from the induced term.
- Hover requires more power than forward flight for a limited range of helicopter speed. This is mainly due to the decrease in induced velocity in forward flight conditions, which in turn reduces the induced power term.
- There exists a forward speed for which the required power is minimum. It can be either found graphically or solving for the conditions in which the derivative of the power curve with respect to the dimensional forward speed is zero. This point, represented in the *Figure 3.5* as A, by definition maximizes the fuel consumption rate and thus accounts for the maximum range speed.
- Similarly to the previous comment, there will be a point that maximizes the range. By definition, this point will be that in which the derivative of the product between the power curve and the adimensional forward speed with respect to this adimensional speed, is equal to zero. Graphically, this can be found as the tangency between the power curve and a straight line starting from the origin (point B in *Figure 3.5*).
- Maximum forward speed will be limited by the propulsive capacity of the aircraft. Note how for higher forward speeds, total power is larger than in hover mainly due to the increase in profile and parasitic power. For clarity, these conditions are represented by point C in *Figure 3.5*.

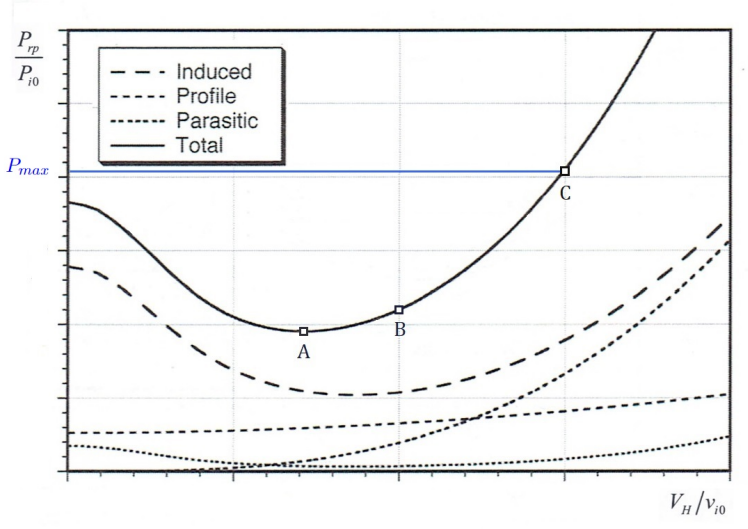

Figure 3.5: Power curve of a generic helicopter as a function of forward speed. Source: Leishman [33].

3.2 Fundamentals of hydrogen-powered propulsion

Next, a brief introduction to the systems involved in hydrogen-powered vehicles will be introduced, giving a comprehensive description and analysis on the different elements as well as the benefits and challenges faced by these systems.

3.2.1 Fuel cells: working principle and architecture

Fuel cells are a type of power generation system based around "redox" reactions in which the chemical energy of a fuel, commonly hydrogen, is converted cleanly and efficiently into electrical energy. Redox reactions are named after the pair of individual chemical processes occurring: the fuel is oxidized, losing electrons that are gained by the oxidizer, which in turn reduces in the process.

Over their history, many varieties of fuel cells have been developed in order to better adapt to their specific application, but the basic design always follows the same pattern, observed in *Figure 3.6*

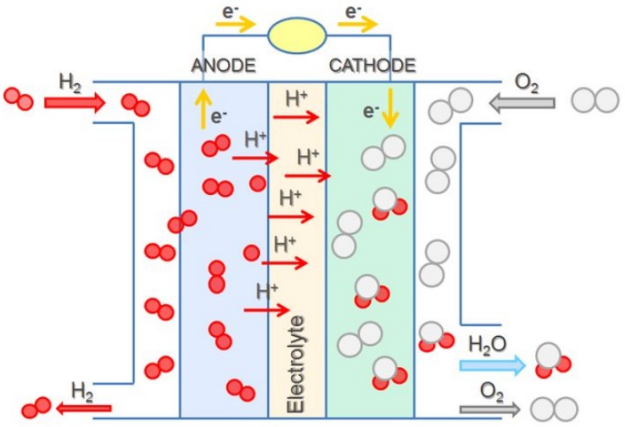

Figure 3.6: Basic scheme of a hydrogen-oxygen fuel cell. Source: Escudero-Escribano [20].

In the first part, called "anode", the fuel is split under the presence of a catalyst, turning into a positively charged ion and losing electrons. Given that the electrolyte membrane only allows ions to pass through, the electrons are then forced to go through the electric circuit creating the current used to power the loads. As they exit the circuit and reach the cathode, thus producing an electric current, they are reunited with the oxidizer.

In the case of hydrogen the reactions are, in general[1]:

$$\begin{aligned} \text{ANODE:} \quad & H_2 \longrightarrow 2H^+ + 2e^- \\ \text{CATHODE:} \quad & O_2 + 4e^- + 4H^+ \longrightarrow 2H_2O \\ \textbf{OVERALL:} \quad & \mathbf{2H_2 + O_2 \longrightarrow 2H_2O} \end{aligned}$$

[1]Note that depending on the type of fuel cell used, based on its architecture (and specially the electrolyte), the reactions vary. This chemical formula is related to solid oxide fuel cells and was chosen for its simplicity.

For most applications, however, fuel cells cannot only consist of just an anode/ cathode pair (single cell), since the electrical power generated would not be enough. Instead, they form a compound system called "stack" in which they are disposed in successive layers, increasing the overall power output of the system.

The fuel cell is the heart of the power generation system, but many other components are required to maintain the correct working conditions for the fuel cell and ensure reaction products exhaust the system properly. *Figure 3.7* shows an example of the integration of the fuel cell stack as the power generator for a propulsive application. In this design, wet air is supplied with the hydrogen through the anode to the fuel cell. The water vapor generated as a product at the cathode outlet is used in the humidifier through which the absorbed air passes before it is released into the environment. Finally, the fuel cell stack not only powers its application but also may provide power for the rest of the components inside the system.

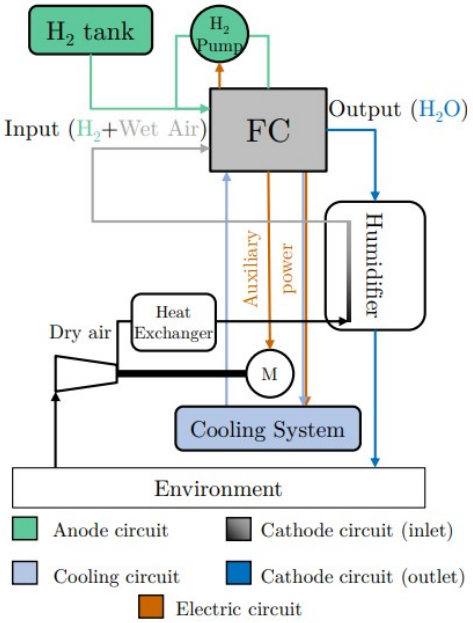

Figure 3.7: Fuel cell system outline. Source: Desantes et al. [15]

As it can be observed, the proper design of a fuel cell system is complex enough in itself. As such, already developed state-of-the-art fuel cell system models were used in this project to accurately predict the fuel consumption of the propulsion system. Nonetheless, since the scope of this project is not the modeling of the fuel cell system, but rather the application of this technology for the aerospace sector, this section will not go into more detail on this topic, but it is helpful to have in mind the systems that will be worked with further on.

3.2.2 Hydrogen storage systems

In order to efficiently store a relatively large mass of such light gas as hydrogen, its density needs to be increased. Under normal atmospheric conditions, pure hydrogen is 11 times lighter than the air we breathe. For perspective, this would mean that 11

m^3, approximately the size of the trunk of a large utility vehicle, are needed to store 1 kg of hydrogen in atmospheric conditions, which would allow you to drive only 100 km in current hydrogen-powered cars. Two approaches can be taken in order increase the density of this compound: storing it as a pressurized gas or, going even further, as a liquid under cryogenic conditions.

Gaseous storage involves pressurizing hydrogen up to 400-700 bar, where its density is increased approximately by 200-400 times respectively. These conditions allow for much more convenient storage volumes for most applications. The tanks used in these cases must have optimized shapes and materials to overcome the extremely high internal pressure without deformations. Typical applications are made of highly resistant metal alloys and composites such as fiberglass/aramid or carbon fiber with a metal matrix like aluminum or steel.

Gaseous storage is very efficient in stationary and road transport applications, but in the case of fuel cell-powered aerial vehicles where long and irregular operation cycles happen, this results in an increase in the overall volume and weight of the storage system, which can become a challenge depending on the case. For this reason, liquid hydrogen storage systems have been developed and are still a big focus of the industry. Under 32 K (-241 °C) of temperature, hydrogen is a liquid with a density more than 700 times higher than under normal conditions, allowing for a reduction of the storage volume of approximately 40% compared to its gaseous counterpart. However, reaching and maintaining this temperature can be very challenging in terms of energy requirements and materials to be used. Currently, these methods are reserved for special applications where volume reduction is especially critical for the feasibility of the application.

Research in this field is specially dedicated to the optimization of current storage technologies and the development of the so-called "materials-based hydrogen storage", where hydrogen could be dissociated into atomic hydrogen inside a metal lattice structure, allowing for low pressure and normal temperature storage with a high volumetric density.

3.2.3 Potential and limitations

Hydrogen as a fuel offers numerous advantages as an energy carrier: carbon-free emissions when used in a fuel cell is the most impactful at an environmental level, but also different production strategies and higher lower heating value makes it very convenient for a wide range of applications, including aerospace. In terms of durability, fuel cells show similar if not somewhat improved performance than electric batteries and they have proven to be very flexible in terms of installation and operation, albeit the efficiency of fuel cells is lower than that of batteries. Furthermore, different from storing electricity in batteries hydrogen storage permits generating permanent stocks of energy in the form of hydrogen, which can be later used to obtain thermal or electrical energy.

However, hydrogen-powered systems have set a series of new challenges that cannot be overlooked. For fuel cells, even if they are not a new concept, commercial applications have only been developed recently, and reliability data show that under certain temperature and humidity ranges, fuel cells suffer premature degradation in comparison to conventional engines [6], [41].

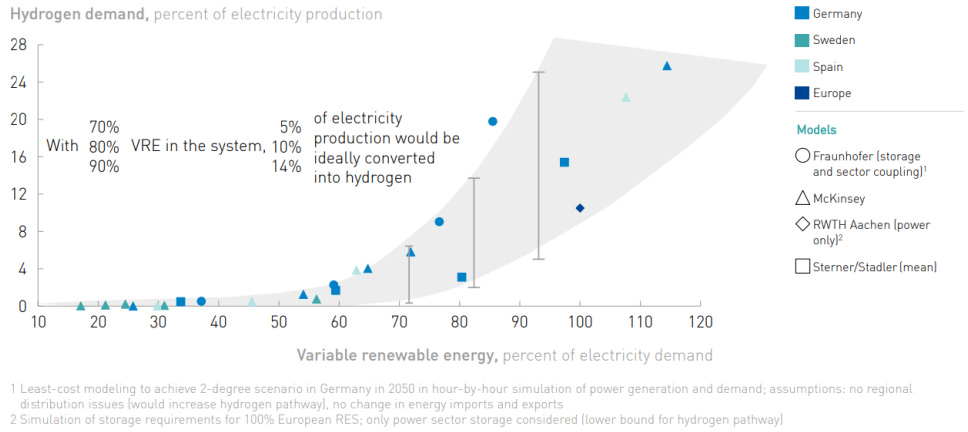

Figure 3.8: Study results of power system simulations with increasing variable renewable energy share, showing the gap that could be cleanly converted into hydrogen. Source: Fuel Cells & Hydrogen Joint Undertaking [2].

As for hydrogen in general, from its production to its consumption, a wide range of problems need to be solved before it can be as widespread as other alternatives. For once, current cost-efficient hydrogen production methods based around methane gas steam reforming have proven even more polluting than common hydrocarbon use [27], [44]. Alternative methods based on electrolysis, which do not produce harmful pollutants by themselves, are in turn approximately seven times more expensive in the short term than readily available fossil fuels [46] and they do require electricity that may come from other not so eco-friendly sources.

Furthermore, current infrastructure for hydrogen production, storage and distribution cannot yet support its widespread adoption and while costs are decreasing, the commitment in the form of necessary investments to propel the use of this technology is uncertain, and with good reason. As Romm [46] so eloquently explains, the market is currently trapped in the need of developing infrastructure to put FCVs in circulation, but it also needs these vehicles to be in circulation to have a good reason to invest in infrastructure.

However, there is good reason to be optimistic in the future development of the hydrogen infrastructure, as two trends are growing as market drivers: the decrease in renewable energy cost and the increasing demand for electricity [57]. As renewables slowly continue to increase their overall share in energy production, the supply chain may exhibit increased short and long-term variations (typical of wind and solar energy production) that could be balanced through hydrogen production, basically absorbing excessive generation in periods like summer and providing power in periods of low renewable production but high energy demand like winter. Different studies, shown in *Figure 3.8* have demonstrated that with elevated shares of renewable energy production, considerable amounts could be ideally converted[2] into hydrogen. This is the main reason different organisms like the European Union are considering hydrogen originated from renewable sources (commonly called *green hydrogen*) as the most viable alternative for future energy supply, even with the technical and economical challenges it represents.

[2]Net conversion of excess renewable energy from the grid into hydrogen.

Chapter 4

Helicopter design adaptation

The core of the project will now be covered in this section, whose main objective is to present the previous work on which the adaptation will be based, as well as introducing the methodology followed to achieve it. The results will be presented for four different applications: one for a one-passenger helicopter, another one for a UAV and two re-adaptations of the first case, studying its behaviour as an UAV and as a two-passenger commuter. Finally, a series of aerodynamic, constructive and economic considerations will be presented, with the objective of setting up future steps in the development of these vehicles.

4.1 Starting point

As previously introduced, the objective of the project is the adaptation of a light helicopter design to introduce a fuel cell power system while maintaining its functional purpose. In order to do so, the model obtained by Tejada in his BSc thesis "Diseño conceptual de un *Light Helicopter* para trabajos aéreos" [56] was kindly provided.

The concept is a first approximation for a light helicopter with very similar characteristics and objectives to this project. The result was obtained through a statistical study of similar aircraft, mainly formed by recreational purpose light helicopters like the already mentioned Dynali H2 or the RotorWay A600. Additionally, in the case of weight approximations, models such as those proposed by Prouty [42] or López Ruiz [36] are used to obtain the distributions among elements, and compare these results to the estimated propulsive requirements. Note that the powerplant chosen for the resulting model, with an approximate MTOW around 450 kg, was the internal combustion engine *Rotax 914*, used in a wide variety of aerospace applications. The obtained dimensions and weight distribution are reflected in *Figure 4.1* and *Table 4.2*, respectively.

As for the aerodynamic properties, the blade profile was selected according to its desired application and resulted in the NACA0012. Other related values were obtained from the study in order to calculate the rotor characteristics, following a methodology out of the scope of this project, and will be useful to considerate for in the analysis too. All

of these values are gathered in *Table 4.1*[1].

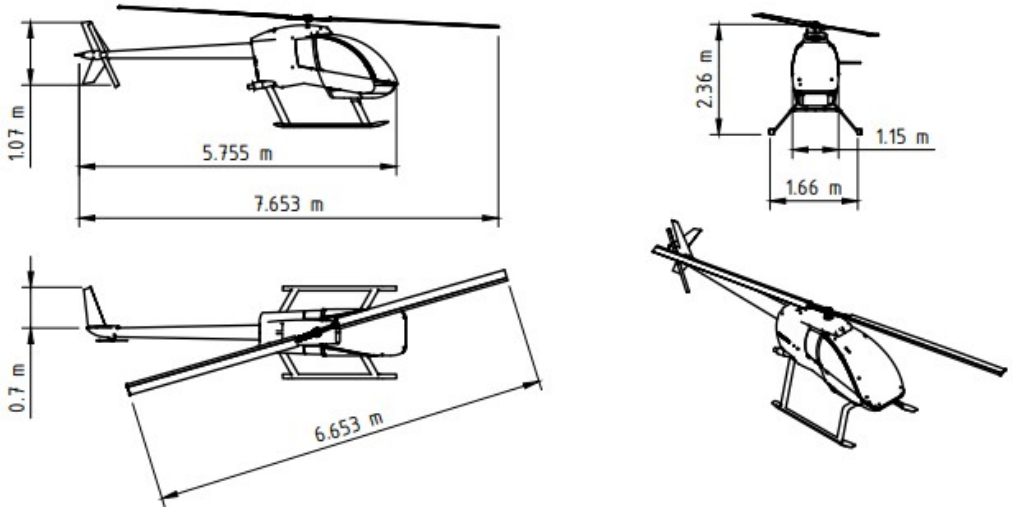

Figure 4.1: Dimensions obtained by Tejada [56] for the light helicopter based on a similar aircraft analysis.

Parameter	Symbol	Value	Units
Tip mach number	M_{tip}	0.544	-
Number of blades	b	2	-
Solidity	σ	0.04	-
Chrod	c	0.209	m
Profile drag coefficient	$C_d = \delta_0 + \delta_1\alpha + \delta_2\alpha^2$	$0.00538 - 0.0184\alpha + 0.451\alpha^2$	-
Lift curve slope	a_t	6.274	rad^{-1}
Flat plate equivalent surface	f	0.3254	

Table 4.1: Summary of aerodynamic parameters of the main rotor and fuselage obtained by Tejada [56] that are relevant for the adaptation performed in the project.

The idea will be, according to the objectives of this project, to maintain this overall structural dimensions but recalculate the requirements introducing a fuel cell as the power generation system. This will also involve the substitution of the weight reserved for fuel, as that parameter will also be affected by the newly calculated hydrogen tanks, and the electrical system, which originally consisted of the battery and electrical distribution and will also be estimated according to the new adaptation as it is expected that the battery will take part in the takeoff procedure for the new helicopter.

It is also important to consider the changes in the mass of the structural elements as the helicopter changes its own mass, since they were originated from statistical approximations mainly based around this parameter. Following this methodology, the original mass of the structure and miscellaneous elements will be adapted as to maintain coherence between this starting point and the final results.

[1]Note that tail rotor data will not be used in the adaptations since they will be focused on the power calculations for cruise or takeoff, situations dominated by the main rotor. Instead, simplifications will be made to estimate its power consumption and movement

Element	Mass [kg]
Main rotor	56.00
Tail rotor	6.50
Fuselage	25.00
Landing gear	6.75
Engine*	78.00
Fuel*	44.20
Instrumentation	1.50
Transmission**	25.00
Hydraulic system	5.50
Electrical system*	30.00
Avionics	15.00
Passangers	145.00
Cabin controls	5.20
Tail structure	6.35
Other equipment	5.00
Total	**450,00**

Table 4.2: Weight distribution between elements obtained by Tejada [56].
* Elements related to the previous power system that will be substituted.
** Elements that will be removed from the new model and thus are not relevant for the scope of this project.

As another design characteristic of the adapted version, it will be calculated with the removal of the transmission system in favour of having one electric engine dedicated for each rotor, as this is estimated to reduce the total weight of the aircraft given the lower power requirements of the tail rotor. Finally, an estimated 7.5 kg for the required connections between electrical elements within the propulsive system will also be considered.

4.2 Methodology

Once the initial conditions for the model are set using the corresponding sources, the method used to perform the adaption will be thoroughly described. More specifically, the main points to develop will be to obtain the new characteristics for the structure, fuel cell, fuel storage system and electrical motors. Starting from the mission definition and cases to study, focus will shift towards a schematic overlook at the different stages of the iterative procedures, the data used to perform the estimation will be provided, as well as the reasoning underlying the decision-making. After having described the procedure in general terms, a deeper dive into the mathematical models, assumptions and consequences of each part of the dimensioning of the elements will be made.

4.2.1 Description of the different case studies and mission objectives

Before going any further, it is worth introducing the different variants to be calculated. Mainly, two versions of the helicopter are desired: a one-passenger model (each passenger with an average mass of 70 kg [60]) and a remotely-controlled unmanned variant. The reasoning behind this decision is simple: reach valuable results for the two main rising branches of application as well as contrast the difference between the two models and the implications on the powerplant and storage system dimensions, obtaining details on the implications of increasing the payload on these type of applications. Each model will be expected to also hold an additional payload of 30 kg[2], reserved for cargo or equipment related for its own application. Finally, note that, in the case of the UAV, the cabin controls will no longer be necessary and thus their weight will also not be accounted for.

The mission to used to estimate these models was selected according to the already observed market needs: being able to perform both urban and inter-urban commutes efficiently and with enough flexibility to be economically viable. Based on developing projects and according to the opinion of experts on the electric vehicle market [51], a target range of 300 km at a cruising altitude of 500 m (common value according to a similar aircraft study [56]) will be established, allowing the aircraft to perform at least one flight between urban nuclei as well as a good number of urban commutes without the need to refuel. Additionally, a minimum of 5 m/s of ascent velocity will also be a mission requirement in order to ensure its competitiveness regarding conventionally-powered prototypes of light helicopters.

Extending on this topic, it will also be calculated, as more of a thought experiment, what would be the result of adapting the one-passenger variant in order to allow for two passengers without changing the powerplant. In principle, it is very likely that the dimensioned powerplant for the first application does not allow this one to take-off, so in order to fix the weight to the original, mass will actually be taken away from the storage system and the additional payload, resulting in an approximation of the actuations of this variant. This will also allow to conclude if the range and endurance of this model are suitable for air taxi applications. Alternatively, the opposite case will be studied in order to find out the potential of Model B if it was to be remotely controlled.

According to this description, the four variants to be calculated are summarized in *Table 4.3*

	Model A	**Model B**	**Model C**	**Model D**
Passengers [-]	0	1	2	0
Mass of the passengers [kg]	0	70	140	0
Cargo [kg]	30	30	0	30
Reduced fuel capacity?	No	No	Yes	No
Range objective [km]	300	300	*	**
Ascent speed [m/s]	5	5	5	5

Table 4.3: Characteristics of the three variants to be calculated in the study.
* Maximum allowable with the reduced tank capacity.
** Maximum allowable with the reduced payload.

[2]Additional cargo capacity based on maximum aircraft hold luggage allowed in commercial applications and common helicopter surveillance equipment weight [32].

4.2.2 Complete iterative procedure overview

The methodology followed in order to perform each case study can be summarized through *Figure 4.2*, whose initial inputs are the fixed weights and the missions already described in previous sections.

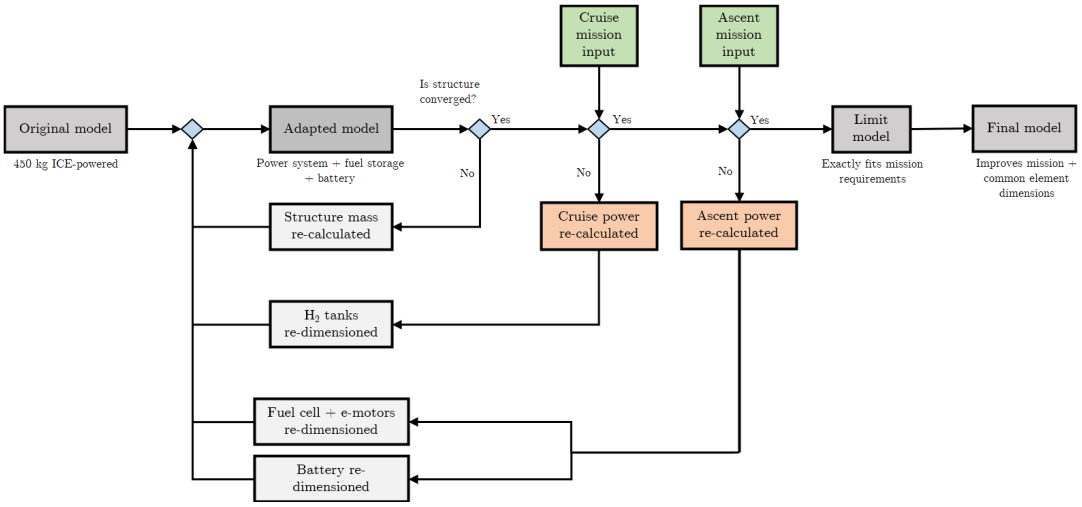

Figure 4.2: Flowchart of the overall procedure followed to perform the helicopter adaptation.

The procedure is predominantly formed by three dependent loops. The first one, called from this point on the **structure loop** focuses on adapting the masses of the structural and miscellaneous elements of the helicopter according to the corresponding mathematical correlations [42]. Once done, the **cruise loop**, will be used to calculate iteratively the fuel reservoir characteristics needed to complete the mission given the components specified for that iteration, settling the complete mass of the aircraft for a given case of the power elements. The third loop, called **ascent loop**, will use the previous results in order to estimate the power required to take-off and ascend at different rates with the previously obtained weight distribution and determine if the power available to the aircraft is enough to perform the maneuver specified. From this result, the fuel cell and motors power will be updated. Additionally the battery size will be determined since it is expected that it can be used to provide, if needed, the difference between the required and the fuel cell system supplied power. The weight of the complete aircraft will therefore be updated given the new dimensions of these elements and thus, the structure and later cruise power will required new updates, repeating the complete process until convergence.

Starting in the structure loop, the conditions to be first introduced are: the so-called "fixed mass" (m_0) of the aircraft corresponding to the structural and miscellaneous characteristics, the "payload mass" (m_{PL}) corresponding to the payload[3], the "power devices mass" (m_{PD}) and "fuel storage mass" (m_{FS}) corresponding to an estimated mass of the fuel cell, motors and battery and fuel storage system respectively.

$$m_H = m_0 + m_{PD} + m_{PL} + m_{FS} \tag{4.1}$$

[3]Including both cargo and passengers

Regarding m_{PD}, the different masses that compose it will be calculated at the beginning of the iteration from empirical relationships between nominal power outputs and component mass according to the current state of the art in electric motors and fuel cells. In a similar manner, the mass and volume of the hydrogen tanks can be estimated from their current gravimetric and volumetric densities. These parameters are gathered in *Table 4.4*. For the initial iteration, an estimation of the required powers and fuel masses will be arbitrarily chosen based on the results obtained by Tejada for the cruise flight of his model, in order to obtain a first result for the complete mass of the adapted aircraft, which will be then turned into one of the inputs needed to calculate m_0 again as described in *Section 4.2.3*, iterating until convergence.

Parameter	Value	Units
Fuel cell system specific power	1.65	kW/kg
Electrical motor specific power	0.65	kW/kg
Battery energy density	35	kWh/kg
H_2 **tank gravimetric capacity (liquid)**	0.20	$kg\ H_2/kg\ system$
H_2 **mass lower heating value**	33.33	$kWh/kg\ H_2$
H_2 **volume lower heating value (liquid)**	1,600	$kWh/m^3\ H_2$
Liquid H_2 **density**	70.85	kg/m^3

Table 4.4: Parameters used to obtain the masses related to power devices and the fuel system. Sources: U.S. Department of Energy [16], Olszewski [40] and Howell et al. [28].

With the helicopter mass set for a given fuel cell, motors, battery and fuel storage combination, the effect of the hydrogen tanks' dimensions is roughly optimized as described in *Section 4.2.4*, finally adding their contribution to the base model fuselage drag through its own calculated flat plate equivalent surface.

Having the model completely defined in terms of mass and aerodynamics, the required average power to complete a cruise mission with the objective range can be calculated according to *Section 4.2.5*. Note that this result will depend on the velocity, the altitude and the mass of the whole aircraft, which can be assumed to be constant for the whole flight given the actual change in weight due to hydrogen consumption is negligible. The velocity chosen for each iteration will be such that it maximizes the range of the aircraft, except for the first iteration in which an arbitrary initial value will be needed to begin the calculations.

With the average power for the cruise computed, the amount of hydrogen fuel required to complete the mission can be obtained from the total energy consumed according to *Section 4.2.6*. This value is ultimately the result of the product between the average power consumed by the fuel cell and the time required to complete the mission. However, non-ideal behaviour of both the fuel cell system and the electrical motor are to be expected. Additionally, the effects of the power losses at the needed DC/DC transformer, the fuel cell and the electric motors will also be accounted for through the corresponding efficiencies based on current state of the art simulations.

The new amount of hydrogen calculated will serve to update the mass and volume of the fuel tanks. The result of a complete iteration of the cruise loop is a new updated value of the mass of the whole helicopter, which will require the recalculation of the structure mass and ultimately, cruise power again. Iterations will continue until convergence of the aircraft mass is found, at which point the hydrogen tanks and structure are considered

dimensioned for the current iteration. Note that the convergence criteria will be set at a value of 1% of relative error with respect to the previous calculation, as the actual power differences at that level of difference can be assumed negligible.

With this result, the ascent loop begins, in which the power required to ascend to the mission altitude is calculated. The power computed will serve to update the masses of the fuel-cell system and the electrical motors so that they allow for this maneuver[4]. Note that, opposite to the cruise case, power will not be constant, as it will depend on the density of the point at which the ascent power is calculated since the requirement to maintain a constant traction coefficient is imposed. Integrating the resulting curve over time as described in *Section 4.2.7* will result on the energy consumption values derived from the ascent. It is worth noting that the approach to dimension the battery will be to allow it to supply additional power for cases in which the conditions exceed fuel cell capabilities.

Once a final result is achieved, the possibility of assessing the performance of the aircraft using commercially available and compatible components is also possible by following the same procedure one final time.

4.2.3 Estimation of the helicopter structural mass

As the first step towards the model design, it is important to accurately estimate the mass of each individual element not related to the powerplant change. Realistically, these values are the result of many factors such as the mission, configuration or design economy. As a first approximation however, mathematical correlations found in the literature gather and add the effects of different parameters to compute a somewhat faithful approximation from which to continue the design process.

Regarding examples of proposed mathematical models for mass estimation in helicopters, commonly accepted versions are those suggested by Johnson [31] or Prouty [42]. In the case of light helicopters, however, these approximations can output incoherent results since most of the bibliography is centered around conventional helicopters, with masses starting at ten times the estimated objective of this project. After testing the results that each one would output, conclusions were found that Prouty's equations had a better behaviour for the conditions that are being looked for in this project.

Even taking this into consideration, some parameters such as the landing gear or the avionics give very unrealistic results (on the order of 1 kg in the case of the landing gear and up to 30 kg in avionics for a 600 kg of helicopter). To always work within a certain safety margin, the landing gear and avionics masses will be based on Tejada's results for the original model [56]. Additionally, given the characteristics of the model, the electrical system weight approximation cannot be applied since the elements included are being calculated on the side. In the same way, as the transmission system is replaced by a different motor to power the tail rotor, it is not necessary to calculate the mass of the transmission as suggested by Prouty. Instead, the transmission weight is neglected and the tail rotor mass can be calculated as a scaled down version of the main rotor in which

[4]The updated values will be over-estimated by 5% in order to reduce the number of iterations required.

the rotation speed is such that the tip velocity is kept constant[5].

Note that, even with these assumptions, the philosophy of overestimating the weight is very much still in place, since Prouty's correlations are 20 years old, and in the author's own words, "the use of composite materials and advanced technology should result in a weight reduction of some of these components".

In conclusion, the equations being used to calculate the individual structural and miscellaneous (equipment, instrumentation, etc.) are shown next:

- Rotor blades

$$m_{R,b} = 0.026 \cdot b^{0.66} \cdot c \cdot R^{1.3} \cdot (\Omega \cdot R)^{0.67} \tag{4.2}$$

- Rotor hub

$$m_{R,h} = 0.0037 \cdot b^{0.28} \cdot R^{1.5} \cdot (\Omega \cdot R)^{0.43} \cdot \left(0.67 \cdot m_{R,b} + \frac{g \cdot J}{R^2}\right)^{0.55} \tag{4.3}$$

- Fuselage

$$m_{R,h} = 6.9 \cdot \left(\frac{MTOW}{1000}\right)^{0.49} \cdot L_f^{0.61} \cdot S_{wet,f}^{0.25} \tag{4.4}$$

- Hydraulic system

$$m_{Hid} = 37 \cdot b^{0.63} \cdot c^{1.3} \cdot \left(\frac{\Omega \cdot R}{1000}\right)^{2.1} \tag{4.5}$$

- Cabin controls

$$m_{CC} = 36 \cdot b \cdot c^{2.2} \cdot \left(\frac{\Omega \cdot R}{1000}\right)^{3.2} \tag{4.6}$$

- Equipment

$$m_{Ins} = 6 \cdot \left(\frac{MTOW}{1000}\right)^{1.3} \tag{4.7}$$

- Instrumentation

$$m_{Ins} = 3.5 \cdot \left(\frac{MTOW}{1000}\right)^{1.3} \tag{4.8}$$

As a side note, these equations must be used in the imperial system according to Prouty's background. For convenience, these units are summarized in *Table 4.5* with their conversion into the metric system.

[5]This simplification, even if somewhat arbitrary is found to be accepted by most authors [33], [42]

Magnitude	Metric	Imperial	Conversion factor Metric → Imperial
Mass	kg	lb	2.2046
Length	m	ft	3.2808
Surface	m^2	ft^2	10.7639
Power	W	hp	0.0013
Moment of inertia	$kg \cdot m^2$	$slug \cdot ft^2$	0.7376

Table 4.5: Units to be used for Prouty's correlations (imperial) and their conversion from the metric system.

4.2.4 Hydrogen tank dimensioning

The need to find out an overall dimension for the tanks comes from the fact that this value will indeed affect the previously estimated equivalent flat plate area of the aircraft, which is nothing else than a measure of the drag experimented by the hub, fuselage, landing gear and others.

The objective with these calculations is to more accurately predict the effect of the worst case scenario in terms of drag increase due to the addition of the tanks, that is, if they were to be located on the exterior of the aircraft. Working with this negative scenario will give a certain safety range to the power calculations, as the ideal case would consist on a storage system inside the structure which would not cause additional power requirements. Furthermore, inside this worst-case scenario, it would be interesting to obtain a size that is reasonable according to the state of the art and the optimization of the volume to generate the least possible aerodynamic resistance.

The question, then, is how to accurately predict the increase in drag generated by these elements. *Figure 4.3* shows the position of the tanks on the helicopter that will be used to estimate their drag. This position is thought to be the most plausible given that the storage system would need to be distributed evenly on the sides of the fuselage to maintain a similar center of gravity than the original model. The similarity between this position and fuselage-embedded nacelles in an airplane is apparent, so the procedure used to calculate the parasitic drag coefficient of these elements will be used.

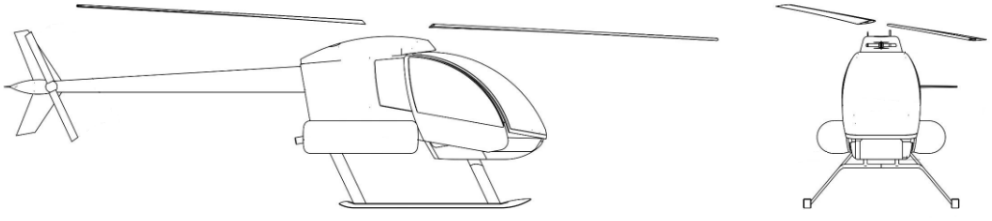

Figure 4.3: Scheme of the exterior tanks position. Adapted from Tejada [56].

The volume of each tank can be calculated from the mass of hydrogen[6] being stored using the values of *Table 4.4* such that:

[6]This value will be, looking at the references on liquid hydrogen storage [64], over-dimensioned by 25% on purpose to account for the additional volume generated by the tank structure.

$$V_{tank} = \frac{1}{2} \cdot \frac{m_{H2}}{\rho_{H_2}} \tag{4.9}$$

The volume will then be structured as a perfect cylinder (as this is the most common shape) of radius R_{tank} and length L_{tank}. Next, for the given flight conditions (mainly density and velocity, as viscosity is assumed constant for the flight domain of the aircraft), the Reynolds number is calculated. Note that the Reynolds cut-off number is also estimated using Roskam's [47] approximate expression[7], and the lower of the two is used for the following calculations as another preventive measure for the calculations (a lower Reynolds number will yield higher drag results).

$$Re = \frac{\rho \cdot V \cdot L_{tank}}{\mu} \qquad Re_{cut-off} = 38.21 \left(\frac{L_{tank}}{k} \right)^{1.053} \tag{4.10}$$

With this parameter, the parasitic drag coefficient can be estimated, using the more common interpretation gathered by Roskam, the product the friction coefficient (*Equation 4.11*, by White-Christoph [63]), the form factor (*Equation 4.12* for circular cross section elements [47]) and the interference factor, which according to Shevell [52] it is around $Q_{tank} = 1.3$ for fuselage mounted nacelles, all weighed through the wet to reference area ratio.

$$CF_{tank} = \frac{3.91316}{(1 + 0.144M^2)^{0.65}[ln(Re)]^{2.58}} \tag{4.11}$$

$$FF_{tank} = 1 + \frac{0.35}{L_{tank}/D_{tank}} \tag{4.12}$$

Therefore, the final expression is given in *Equation 4.13*:

$$(CD_0)_{tank} = CF_{tank} \cdot Q_{tank} \cdot FF_{tank} \cdot \frac{S_{wet,tank}}{S_{ref}} \tag{4.13}$$

where the reference surface is, in this case, the rotor area.

Using Leishman's [33] definition of the equivalent flat plate area, and from the previous result, the value of f_{tank} can be calculated and added to the result of the original model.

$$f_{tank} = (CD_0)_{tank} \cdot S_{wet,tank} \tag{4.14}$$

In order to optimize the dimensions of the tank and choose a final result, the objective will be to minimize the value of f_{tank} for a given overall tank volume. Given the simplicity of the shape, either the diameter or the longitude of the tank is taken

[7] Note that there exists an alternative expression for the case in which the Mach of flight is higher than the critical Mach, but these conditions are not going to be met by the aircraft

as a variable, fixing the other one to maintain the correct estimated volume, and the calculations can be performed as described to obtain this minimum. Take, for instance, the case described in *Figure 4.4*, in which, for a liquid hydrogen mass of 5 kg, the corresponding volume of the tank is estimated to be $88L$ and the equivalent flat plate area as a function of the tank diameter is shown, finding the minimum at a value equal to, approximately $d_{tank} = 0.38m$.

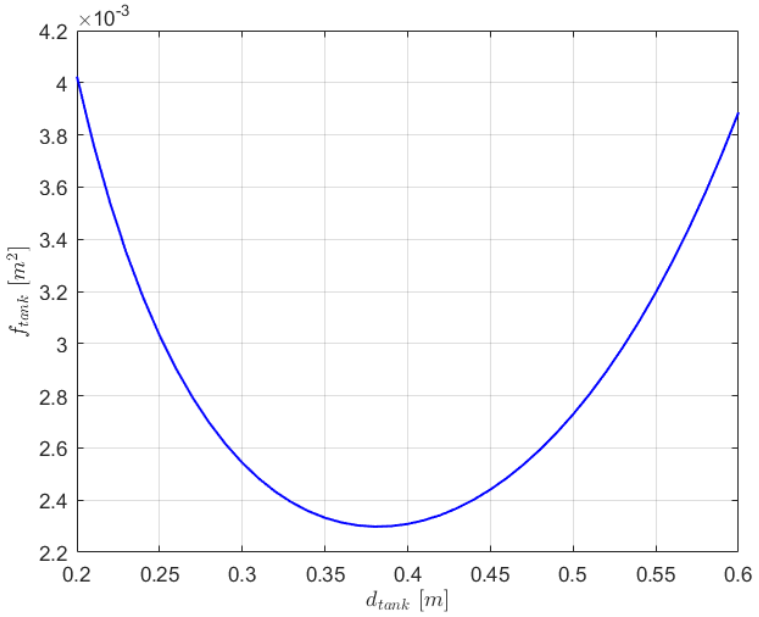

Figure 4.4: Equivalent flat plate area of a tank of $0.12m^3$ as a function of the tank diameter (sea level altitude and $V = 100km/h$)

Results found by previous studies on helicopter drag suggest that the increase in drag caused by the placement of external tanks should range from 2 to 6% [33], [45], [55] depending on many factors, such as distance to the fuselage, frontal area, type of element or air stream conditions. This procedure yields lower results (1-2%), which is to be expected given their optimized shape, and better correlates with that expected of actual fuel tanks and not engine nacelles.

4.2.5 Main rotor cruise power calculation

In order to estimate the power required in cruise conditions, each of the components will be calculated independently according to the theoretical background previously developed.

For induced power, the result is directly obtained from momentum theory. After applying the correction factors B and κ for compressibility effects and tip losses, by definition

$$P_{in} = \frac{\kappa}{B} \cdot T \cdot v_i = \frac{\kappa}{B} \cdot T \cdot v_{i0} \cdot \frac{\lambda}{\lambda_0} \tag{4.15}$$

All of the terms expressed on *Equation 4.15* are easily obtainable from momentum theory and blade-element analysis. On one side, the thrust value is approximately equal to the weight ($T \approx W$) for small angles of attack. The correction factor for tip losses B can be approximated through a simplified model to $B = 1 - \sqrt{2 \cdot C_T}/b$, with the value of the thrust coefficient being calculated through *Equation 4.16*, from which all the values are known except for the rotational speed of the blades. The regression found by Tejada [56] will be used in this case, having $\Omega = (0.0002 \cdot m_H + 0.4526) \cdot a/R$ at sea level[8]. Finally, $\kappa \approx 1.15$ is a commonly accepted value for preliminary power calculations based on empirical results [33].

$$C_T = \frac{T}{\rho \cdot S \cdot (\Omega R)^2} \tag{4.16}$$

Finally, the induced velocity is calculated from traditional momentum theory, starting from its value of the in hovering conditions (*Equation 4.17*)

$$v_{i0} = \sqrt{\frac{T}{2 \cdot \rho \cdot S}} \tag{4.17}$$

Defining the "advance ratio" and the "inflow ratio" through *Equations 4.18* and *4.19*, the induced inflow equation is solved iteratively as shown in *Equation 4.20*, usually using the inflow ratio for hover conditions ($\lambda_0 = \sqrt{C_T/2}$) as the initial value.

$$\mu = \frac{V \cdot cos\ \alpha}{\Omega R} \tag{4.18}$$

$$\lambda = \frac{V \cdot sin\ \alpha + v_i}{\Omega R} \tag{4.19}$$

$$\lambda_{n+1} = \mu \cdot tan\ \alpha + \frac{C_T}{2\sqrt{\mu^2 + \lambda_n^2}} \tag{4.20}$$

This equation is said to have converged if the relative error is below 0.05%. Note that the angle of attack (which for momentum theory is the helicopter tilt) can be assumed zero to further simplify the solution, but far more realistic results are obtained from using similar aircraft results, which in general take values between 1°-5°. This value will be approximated following *Equation 4.21*, where Θ_0 is the value to calculate now that all of the values are known, except the blade angle of attack which will be set to a common value of 1.5°[56].

$$C_T = \frac{1}{2} \cdot \sigma \cdot C_{l\alpha} \left(\frac{\Theta_0 - \alpha_0}{3 - \lambda_0/2} \right) \tag{4.21}$$

[8]Note that, for altitudes other than sea level, this rotational speed is corrected in order to maintain a constant traction coefficient at different air density

For blade profile power losses, after considering the resistance generated by the blade advance and rotation as well as the reverse flow region, *Equation 4.22* (obtained from blade-element analysis [33]) can be used:

$$P_0 = \rho \cdot S \cdot (\Omega R)^3 \cdot \left(\frac{C_{d0}\sigma}{8}\right) \cdot \left(1 + 3\mu + \frac{3}{8}\mu^4\right) \tag{4.22}$$

In the case of parasitic power losses, using the definition of the flat plate equivalent area (updated with the influence of the tanks) the result can be summarized in *Equation 4.23*:

$$P_f = \frac{1}{2}\rho V^3 f \tag{4.23}$$

The complete expression will therefore be the sum of its components, reflected in *Equation 4.24*.

$$P = \frac{\kappa}{B} T v_{i0} \frac{\lambda}{\lambda_0} + \rho S (\Omega R)^3 \left(\frac{C_{d0}\sigma}{8}\right) \left(1 + 3\mu + \frac{3}{8}\mu^4\right) + \frac{1}{2}\rho V^3 f \tag{4.24}$$

Comparing the different components of the power is interesting, since it is possible to check the accuracy of the method by looking at the similitudes[9] between *Figures 4.5* and *3.5*.

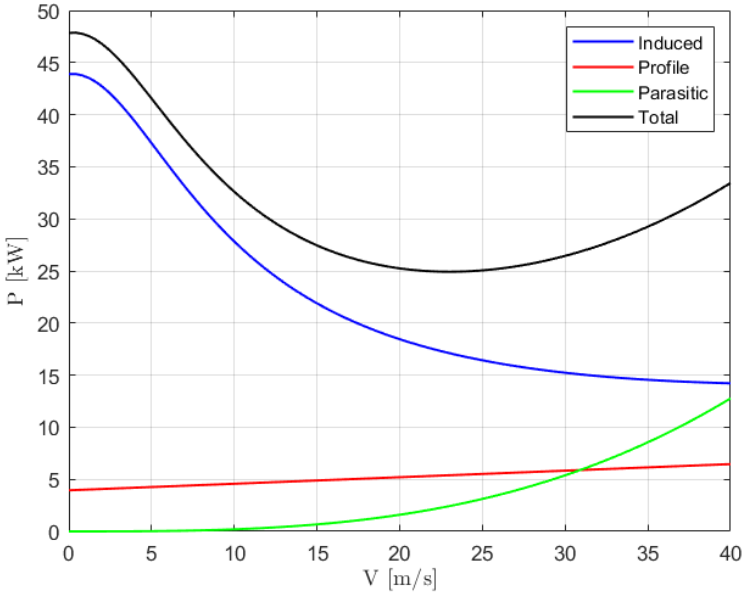

Figure 4.5: Power estimations for the main rotor in cruise flight at sea level for a helicopter with the presented characteristics and 500 kg in mass.

[9]Note that the low velocity region should not be considered accurate since some of the assumptions made to reach the resulting formulas depend on high-speed approximations.

The only question left to estimate the power of the mission is to determine the most appropriate velocity, which in this case is one such that volume is maximized. As previously introduced, this result can be estimated by making use of the power curve of the helicopter, given by *Equation 3.2*. To simplify the derivation required, the high speed approximation will be used.

4.2.6 Fuel requirement

While the previous section allows for the calculation of the required main rotor power, the fuel cell will need to supply additional power given several losses in the system. More especifically, non-ideal efficiency of the following elements will be assumed:

- **DC/DC converter**: According to the bibliography [54], it is expected that current state of the art converters have an estimated efficiency of $\eta_{DC} \approx 0.95$.
- **Electrical motor**: It is well known that the power losses of these motors are directly correlated to torque specified. While in a first approximation it can be assumed that $\eta_{EMotor} \approx 0.95$, the results will be improved using data obtained through operation maps kindly provided by López Juárez for differently-sized electrical motors. Represented in *Figure 4.6*, these data can be found for electric motors of 80 and 100 kW respectively.
- **Fuel cell**: Current fuel cell models are able to convert into electrical power approximately only 50% of the energy stored by hydrogen ($\eta_{FC} \approx 0.5$), being this efficiency affected by the working altitude and the power requirement. Again, this result is a good estimation on its own, but with the objective of more accurately predicting the fuel cell performance, specific data was obtained for the different fuel cell sizes.

  More specifically, dynamic simulations of a 120 kW fuel cell performance at different altitudes were carried out following a state-of-the-art methodology based on the optimization of the air management and the auxiliary power distribution, obtaining not only the fuel consumption efficiency but also specific results in terms of maximum power output [39]. Simulation results are shown in *Figure 4.7*. For results involving the usage of differently sized fuel cells, the power requirement will be scaled to the data used in these simulations such that, even if it is not perfect, the results are clearly closer to that of a real application.

Additional power usage will be calculated at the tail rotor, estimating it as 5% of the power consumed by the main electrical motor according to Rotaru and Todorov [48].

With this, the power supplied by the fuel cell will be given by:

$$P_{FC} = 1.05 \cdot \frac{P_{mr}}{\eta_{eMotor} \cdot \eta_{DC}} \tag{4.25}$$

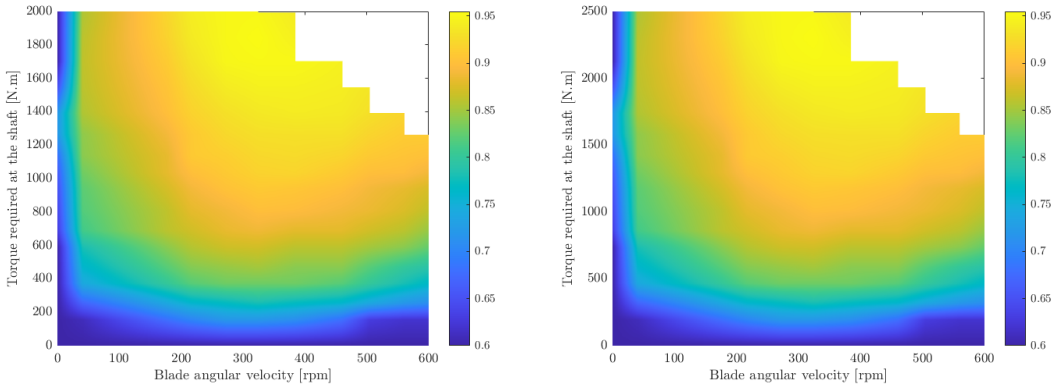

Figure 4.6: Efficiency maps for a 80 kW (left) and 100 kW (right) electric motors as a function of torqu required and rotational speed. Note blank spaces are points not achievable for the motor.

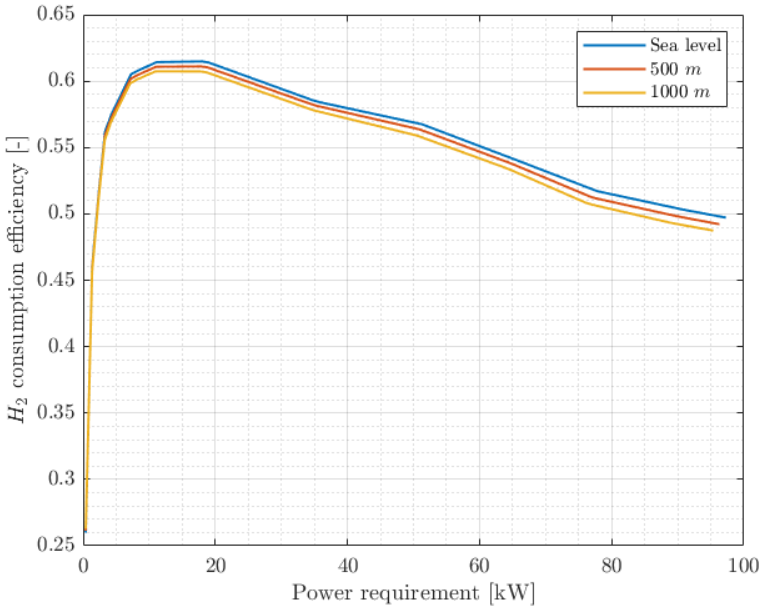

Figure 4.7: Simulated efficiency of a 120 kW fuel-cell as a function of the required power target at different altitudes.

Introducing the fuel consumption efficiency, the the mass of hydrogen required to perform a mission of these characteristics can be obtained through the relationship given by *Equation 4.26* using the values of *Table 4.4*, given that the cruise time is trivial to calculate assuming a constant velocity and the target range specified by *Table 4.3*.

$$m_{H2} = \frac{P_{FC} \cdot t_{Cruise}}{LHV_{H2,mass} \cdot \eta_{FC}} \tag{4.26}$$

4.2.7 Ascending power and energy calculation

In the case of ascending flight at constant speed, the procedure is extremely similar to *Section 4.2.4*, with some relatively small changes to the values of the induced and parasitic components of power.

In this case, the thrust will also need to account for the vertical drag, also commonly known as "download" on the helicopter fuselage. Leishman [33] proposes an equation obtained directly from the combination of momentum theory and the concept of vertical drag for moderate rates of climb, causing the net main rotor power requirements to be equal to:

$$P_{asc} = \frac{W}{1 - f_z/S}\left(\frac{V_z}{2} + \sqrt{\frac{W}{2 \cdot \rho S(1 - f_z/S)}}\right) + P_0 \tag{4.27}$$

where f_v is the equivalent flat plate area for the vertical cross section of the fuselage, different from the one calculated for cruise flight. This value can only be reliably calculated through wind tunnel analysis, so instead a statistical approximation for the ratio $f_v/S \approx 0.05$ is used, since for most cases increases the thrust requirement by 5% [33], [48].

Note that, as mentioned previously, this value of power will not be constant since the rotational speed of the blades will be adjusted to compensate for lower densities at higher altitudes in order to maintain a constant thrust coefficient (take *Figure 4.8* for illustrative purposes). The result will be adjusted through the main motor efficiency in order to give a new value for the required motor power. At the same time, the fuel cell will be affected too, given that it is required to power both motors.

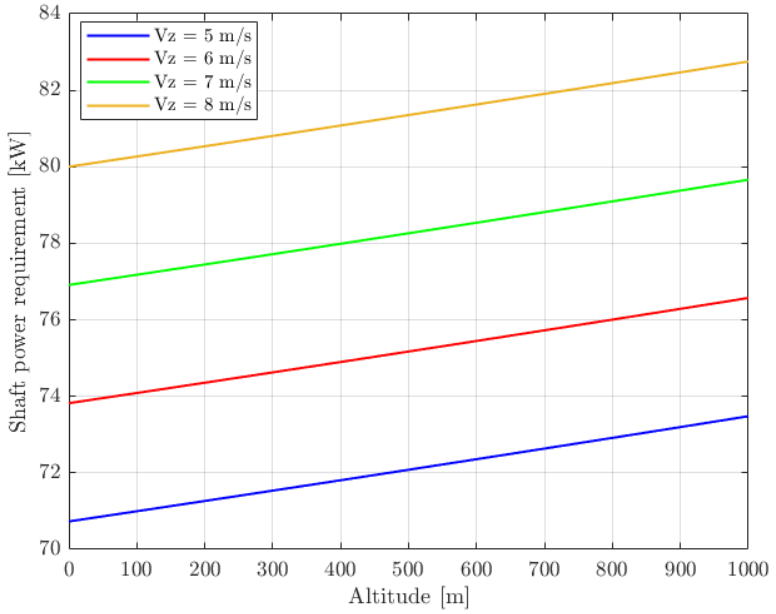

Figure 4.8: Shaft power requirement for the project's design and a mass of 500 kg for different rates of climb.

In an effort to prevent the over-dimensioning of the fuel cell, the battery will be used to provide additional power in specific short periods of time where the requirements exceed the fuel cell capabilities. This approach is particularly interesting given that these situations will mainly happen during the ascent, where the requirements are much higher than in cruise but the time it is required to operate under these conditions is short.

Note that, the maximum effective power suppliable by the fuel (P_{maxFC}) cell is the result of the power losses and the consumption of the auxiliary components of the fuel cell system mentioned in *Section 4.2.5*, as well as other performance limitations that are reflected in the data used to calculate its efficiency [39], ending up in an approximated 20% maximum power output decay when comparing the fuel cell stack maximum power and the fuel cell system maximum power (more specific results can be found through the aforementioned simulations used in this study [39]).

As for how much power the battery is able to provide, the durability of this element is considered essential, thus limitations will be put forward to avoid it working in conditions that may affect its overall useful life. Widely accepted values for safe maximum discharge rate of lithium ion batteries [28] are proposed at 5C[10]. Note that the discharge rate would not be maximum at all points, instead the battery will supply just the required power to perform the maneuver up to this maximum capability, limiting this way undesired discharges or the need to constantly be charging this element.

In conclusion, when the values of the e-motors are updated for the next iteration, there is no work-around and they must fit the hardest mission requirements (*Equation 4.28*). However, in the case of the fuel cell, the power will be reduced such that it is able to give the required energy to the motor until a certain limit at which it is helped by the battery, providing a maximum discharge of 5C (*Equation 4.29*).

$$NP_{main\,eMotor} = \frac{P_{asc}}{\eta_{eMotor}} \qquad NP_{tail\,eMotor} = 0.05 \cdot P_{main\,eMotor} \tag{4.28}$$

$$NP_{FC} = 1.05 \cdot \frac{NP_{main\,eMotor}}{\eta_{FC} \cdot \eta_{DC}} - 5 \cdot E_{Bat} \tag{4.29}$$

Note how for *Equation 4.29*, the left term is equal to the needed nominal power of the fuel cell in case the battery wasn't used and the right term is the maximum power output of the battery.

The total energy consumed, therefore, will not come from the product of power and time but rather the integration of power over time.

$$E_{asc} = \int_0^{t_f} P_{asc} \cdot dt \tag{4.30}$$

[10] A 5C discharge rate would mean that the battery would lose all of its power in 1/5 of an hour. As an example, a battery with a capacity of 2 kWh discharging at a rate of 1C (nominal) would last, effectively 1 hour, meaning the power output is 2 kW. If the discharge rate is doubled, so is the power output

If the battery is only used when the fuel cell requirements exceed its capabilities, the energy required from the hydrogen tanks and from the battery can be independently calculated according to *Equation 4.31*.

$$E_{asc} = (E_{asc})_{FC} + (E_{asc})_{Bat} = \int_0^{t_f} P_{max_{FC}} \cdot dt + \int_0^{t_f} (P_{asc_{FC}} - P_{max_{FC}}) \cdot dt \qquad (4.31)$$

where $P_{max_{FC}} = 0.8 \cdot NP_{FC}$. For the term related to the common hydrogen consumption, the equivalent amount of hydrogen can, again, be estimated through *Section 4.2.6*, while for the battery discharge, a realistic efficiency would be at around $\eta_{Bat} = 0.9$ [30].

4.3 Results

The following section summarizes the evolution of the process followed, concluding in the final results obtained for each of the variants considered for the project, both with bare-minimum design and with commercially available products. Additionally, estimated performace data for the models is displayed in order to obtain a better comparison.

4.3.1 UAV model

Starting with the smaller of the three variants and following the previously described methodology, the UAV model was iteratively calculated.

The whole procedure can be observed in *Figure 4.9*. Note that the internal loops, in which the fuel storage mass and structure mass, where not reflected in the evolution of the mass for clarity,

The results suggest that the combination of elements summarized in *Table 4.6* would yield a model that is able to complete the mission established. These results should be taken as a lower limit size estimation of the elements since by definition, these are the elements capable of carrying out the selected mission but go no further.

Element	Capacity	Mass
Fuel cell	73.75 kW	111.13 kg
Main motor	60.75 kW	37.16 kg
Tail motor	3.03 kW	1.85 kg
Battery	1.50 kWh	8.93 kg
Hydrogen tanks	5.45 kg H_2	27.25 kg H_2 tanks
Total mass of the aircraft: 399.05 kg		

Table 4.6: Summary of elements of the final iteration for the UAV variant.

In order to have a more realistic model, however, one must consider commercially available sizes since for instance, the actual model constructed will not precisely have a

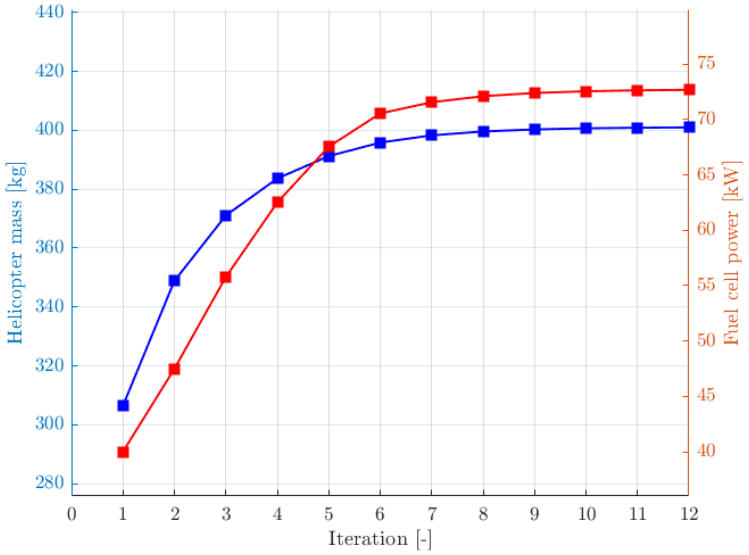

Figure 4.9: Evolution of the UAV design until convergence of the model. Initial values: $NP_{FC} = 40KW$, $NP_{mm} = 30KW$, $m_{H2} = 10kg$.

73.97 kW fuel cell stack. Changing the calculated requirements by alternative elements will influence the aerodynamic performance of the model, so a final iteration is required to not only check that the changes allow for the mission completion, but also to recalculate the overall performance characteristics. In general, the objective will be to round the results up so that the aircraft performance is enhanced, which is specially true for the UAV, since this model will benefit the most from having additional maneuvering capabilities which in turn would translate into a wider range of applications it can be used on.

Based on the previous results, the model resulting from the study is summarized in *Table 4.7*, alongside the rest of the dimensioned structural and miscellaneous elements. From the result of *Table 4.6* to that of *Table 4.7*, the increase in capacity proposed will add flexibility to the maneuvering capabilities of the aircraft as well as power other processes not taken into account yet (external devices, fuel cell start up, etc.) given that the overall weight increase is negligible and should not cause power shortages as the power of the fuel cell has also been increased.

As a first note, the optimized tank dimensions are estimated at a diameter of $d_{Tank} = 0.3$ m and a length of $L_{Tank} = 1.10$ m. This results in a 1.5% increase in the overall drag of the aircraft, which is slightly lower than expected but still within a realistic order of magnitude.

Running the calculations confirms that this configuration is indeed capable of performing the mission in terms of cruise, even allowing for longer trips and higher speeds thanks to the additional power available. The overall actuations of the aircraft are shown in *Table 4.8*. Note, however, that for the case of the maximum speed, results should be taken with caution given that the component of power corresponding to that of the blade movement may not behave as described in the introduced equations as the compressibility effects are expected to be much larger at this velocity.

Element	Capacity	Mass
Fuel cell	80 kW	123.07 kg
Main motor	70 kW	42.81 kg
Tail motor	3.5 kW	2.15 kg
Battery	1.5 kWh	8.93 kg
Hydrogen tanks	2 x 57 L 2 x 3.25 kg H_2	32.5 kg
Fuselage		63.37 kg
Main rotor		69.96 kg
Tail rotor		1.81 kg
Tail structure		6.35 kg
Landing gear		6.50 kg
Hydraulic system		11.93 kg
Avionics		5.00 kg
Power electronics		7.50 kg
Equipment		2.42 kg
Additional payload		30.00 kg
Total mass of the aircraft: 415.72 kg		

Table 4.7: Summary of elements of the UAV model.

		Cruise flight mode			
Parameter	**Cruise altitude**	**Maximum range**	**Maximum endurance**	**Maximum speed**	**Hover**
Rotor Power [kW]	0 m	39.63	28.93	55.00	40.97
	500 m	40.52	29.68	55.02	42.05
	1,000 m	41.57	30.47	54.97	43.18
Velocity [km/h]	0 m	129.90	55.77	170.60	0
	500 m	133.05	56.86	171.80	0
	1,000 m	136.32	57.98	172.70	0
Range [km]	0 m	312.22	171.38	286.82	0
	500 m	307.40	188.56	285.46	0
	1,000 m	302.04	184.96	285.28	0
Endurance [hr]	0 m	2.41	3.45	1.68	2.32
	500 m	2.31	3.32	1.66	2.22
	1,000 m	2.22	3.19	1.67	2.14

Table 4.8: Summary of actuations of the UAV model.

As it can be observed, the vehicle complies with the expected results, since operating in maximum range conditions could allow the UAV to be used for cargo transport between big urban nuclei or long range civil safety and surveillance missions, and reducing the pace would allow, for instance, for urban or maritime surveillance without the need to substitute the aircraft or refuel in the middle of the mission. The power breakdown as a function of the speed can be observed in *Figure 4.10*, where it is clear that the maximum cruise efficiency is achieved at speeds that are indeed very adequate for urban and inter-urban use.

In terms of efficiency, the calculated figure of merit for hover conditions results in 0.71, which is a completely standard value for a common helicopter and could be optimized mainly through a better selection of blade airfoil and shape.

As for the ascent requirements, the aircraft is able to perform as expected without much need of the auxiliary battery power to reach the cruising altitude at the standard

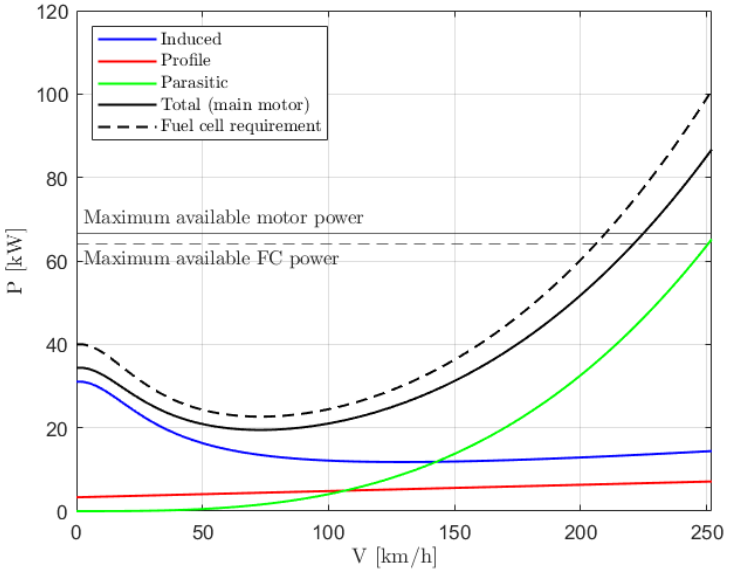

Figure 4.10: Breakdown of power consumption of the UAV model as a function of the flight speed.

rate of ascent established. Analyzing higher ascent velocities and reaching higher altitudes, it can be found that the limiting factor becomes the fuel cell power output, reason why the battery was implemented as previously explained. Using this configuration, the aircraft is able to ascend at the defined mission rate past 1,000 m and even reach the cruise altitude at slightly higher speeds. The rate of discharge is adapted at each point to maximize the battery duration, allowing for instance to perform more than 30 ascents at the mission requirements or 13 ascents at 6 m/s without the need to recharge it or have any concern for its useful life decline.

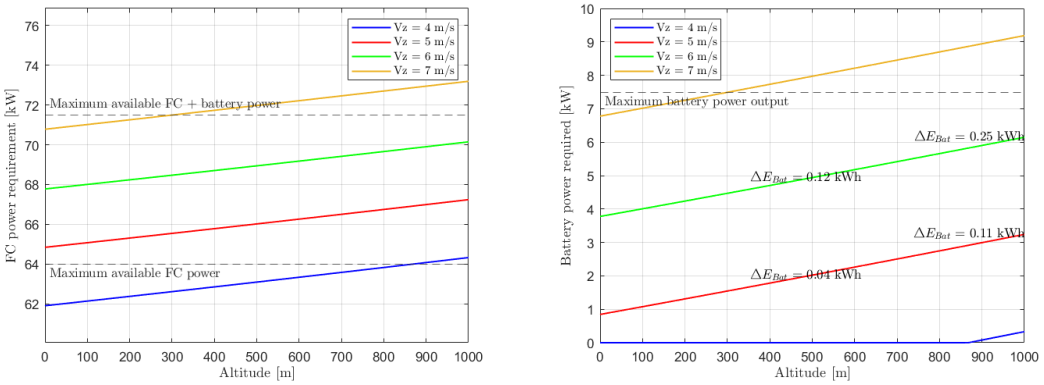

Figure 4.11: Evolution of the power consumed by the vehicle as it ascends at different rates (left) and power required by the battery at each point (right), noting the battery energy consumption at the cruise mission altitude and at its double.

Increasing the payload of the model would cause the aircraft to work under more restrictive conditions but thanks to the slight overdimensioning of the power elements, the UAV could still comply with the ascent mission requirements with double the payload.

4.3.2 One-passenger model

The same procedure can be followed for the model with one passenger, shown in *Figure 4.12*. In this case the addition of an additional 70 kg in mass for the aircraft passenger required a severe increase in the fuel cell power.

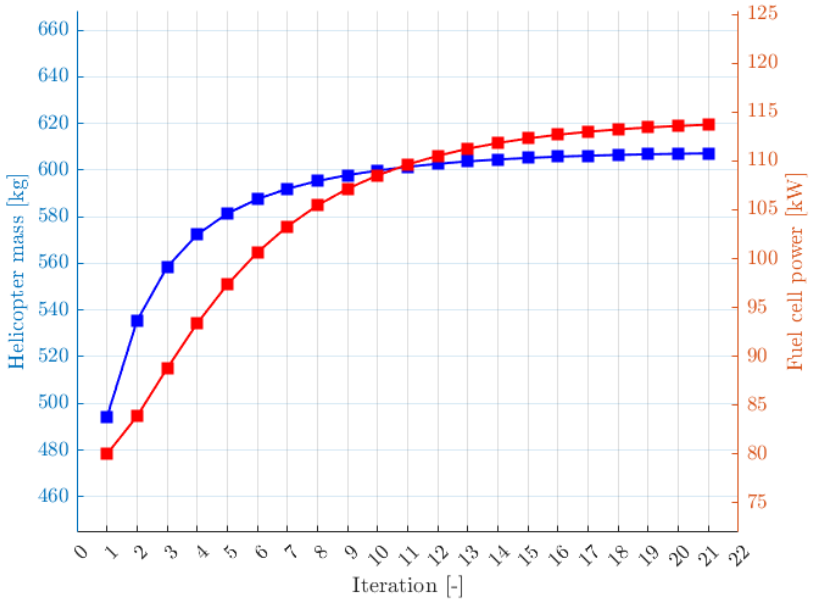

Figure 4.12: Evolution of the UAV design until convergence of the model. Initial values: $NP_{FC} = 80$ kW, $NP_{mm} = 60$ kW, $m_{H2} = 12$ kg.

Again, the combination of elements found in *Table 4.9* are the minimum combination to carry out the required mission under limiting conditions. The same methodology as with the UAV will be used in this case, rounding up the different element dimensions in order to obtain commercially available products and give more flexibility to the design. The model characteristics resulting from the changes are shown in *Table 4.10*.

Element	Capacity	Mass
Fuel cell	117.03 kW	180.05 kg
Main motor	96.78 kW	59.20 kg
Tail motor	4.83 kW	2.96 kg
Battery	1.75 kWh	11.90 kg
Hydrogen tanks	8.75 kg H_2	43.75 kg H_2 tanks
Total mass of the aircraft: 599.71 kg		

Table 4.9: Summary of elements of the final iteration for the one-passenger variant.

The tank dimensions in this case result in an optimal cylindrical shape of $d_{Tank} = 0.34$ m and $L_{Tank} = 1.19$ m, causing an estimated drag increase of 2%, again in the order of magnitude expected.

The model is again able to outperform the mission, this time with a smaller margin given that the overdimensioning of the power elements was smaller. The actuations of the aircraft are calculated and summarized in *Table 4.11*.

Element	Capacity	Mass
Fuel cell	120 kW	184.61 kg
Main motor	100 kW	61.16 kg
Tail motor	5 kW	3.05 kg
Battery	1.75 kWh	8.93 kg
Hydrogen tanks	2 x 80 L 2 x 4.5 kg H_2	45 kg
Fuselage		73.08 kg
Main rotor		71.57 kg
Tail rotor		1.88 kg
Tail structure		6.35 kg
Landing gear		6.50 kg
Hydraulic system		13.83 kg
Avionics		5.00 kg
Power electronics		7.50 kg
Cabin controls		12.07 kg
Equipment		4.00 kg
Pilot		70.00 kg
Additional payload		30.00 kg
Total mass of the aircraft: 608.37 kg		

Table 4.10: Summary of elements of the one-passenger model.

		Cruise flight mode			
Parameter	**Cruise altitude**	**Maximum range**	**Maximum endurance**	**Maximum speed**	**Hover**
Rotor Power [kW]	0 m	64.66	42.21	82.87	67.03
	500 m	66.99	48.91	82.89	69.39
	1,000 m	68.83	50.25	82.95	71.24
Velocity [km/h]	0 m	151.11	63.74	187.5	0
	500 m	155.22	65.11	187.5	0
	1,000 m	159.06	66.37	188.2	0
Range [km]	0 m	314.62	189.92	291.07	0
	500 m	305.81	185.08	287.67	0
	1,000 m	300.35	181.32	285.16	0
Endurance [hr]	0 m	2.08	2.98	1.55	1.99
	500 m	1.97	2.84	1.53	1.89
	1,000 m	1.88	2.73	1.51	1.81

Table 4.11: Summary of actuations of the one-passenger model.

These results are a sign of optimism given that the technology used is able to perform a fairly demanding mission within expectations, and with a figure of merit of 0.75 it can be competitive in terms of aerodynamic performance. The additional payload capacity and its range makes it very useful for private use, either for short commutes or longer trips without the need to fully refuel. Additionally, it can also be used for civil safety or emergency missions given its endurance and projected maximum speed, potentially making it a competitive aircraft to implement with a whole set of environmental benefits not within reach of its competitors, confirming the already expected viability of the concept. Indeed, the power breakdown of this aircraft can be observed in *Figure 4.13*, showing very good performance at adequate velocities for both urban and inter-urban use.

Studying its ascent requirements is perhaps the aspect in which the aircraft is more limited compared to its UAV model. The ascent rate requirement at 5 m/s is clearly the

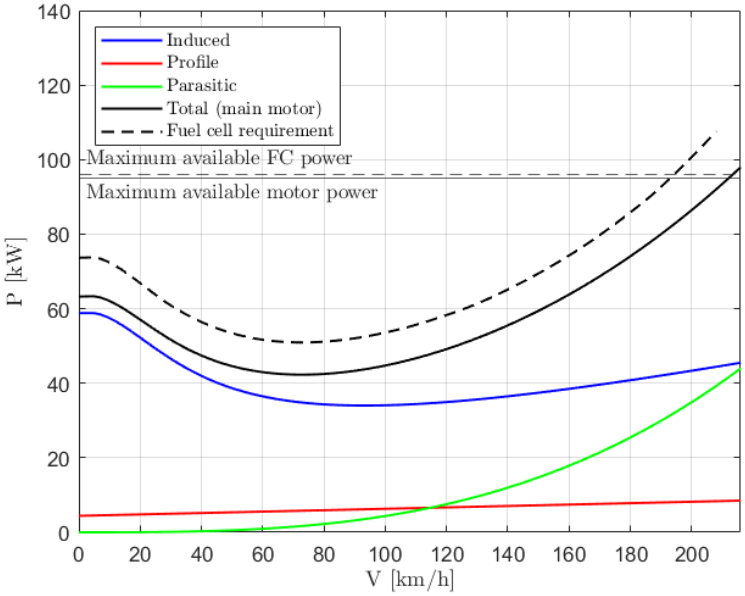

Figure 4.13: Breakdown of power consumption of the one-passenger model as a function of the flight speed.

most demanding for this configuration, since the power needed is already very close to the limit. Using a higher discharge rate of the battery is, as already discussed, not a safe alternative in terms of maintainability of the elements, and using bigger batteries causes the same problem than using bigger fuel cells: an increase in weight and thus an increase in power required. Even for the main electric motor, results show that the maximum allowable ascent rate would happen below 6 m/s. While it is true that a 140 kW fuel cell would allow the model to have a flexibility to operate in ascending segments more similar to the UAV, it is finally discarded since there is not a strong argument to be made that the rate of ascent needs to be any higher than the one established by the mission.

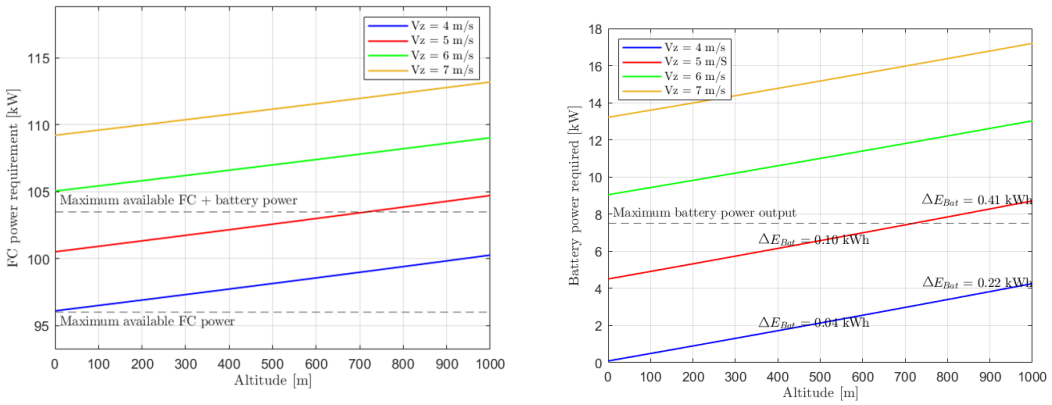

Figure 4.14: Evolution of the power consumed by the one-passenger vehicle as it ascends at different rates (left) and power required by the battery at each point (right), noting the battery energy consumption at the cruise mission altitude and at its double.

As it can be observed, the aircraft is able to reach almost double the cruise altitude but it isn't able to have larger rates of ascent. The battery discharge in this case ranges

between 4C-5C during the whole ascent, which is not worrying because it would take between 1.5 to 2 minutes to reach the desired altitude. This maneuver would allow around 17 ascents to the cruise altitude, which is also a good result taking into account the requirements imposed up to this point.

4.3.3 Variants of the one-passenger model

The next study is thought of as an additional test with the objective of estimating the potential capabilities of different variants of the one-passenger design. Note that the procedure followed is not the same as before, since a new design mission is not being considered.

The first variant to be considered is a reduced-range two-passenger model in which weight is taken off from the payload to make room for the second passenger. From here, two alternatives could be considered: either weight is also removed from the fuel storage system to maintain the same weight and thus maneuvering or the passenger is introduced directly, sacrificing the capabilities of the aircraft mainly for the ascent.

If the choice is made to maintain the same aerodynamic capabilities, given that the weight would be the same, the cruise and ascending power required would be kept constant. The only change would be how long could the aircraft perform given that the fuel has been reduced. For this specific case, removing the payload and reducing the dimensions of the fuel storage until capability for another passenger (again, of 70 kg [60]) is reached, would leave 5 kg for the hydrogen storage system, or equivalently around 1 kg of liquid hydrogen to be consumed. As it can be observed, the price to pay in order to maintain the previously found actuations is a reduced range and endurance.

Both alternatives are compared in *Table 4.12*, where in principle, it would be more tempting to add the second passenger given that during cruise, the designed fuel cell and electric motors are capable of maintaining an acceptable level of performance. The most negative aspect is the maximum ascent rate, which in this case is very low compared to the competition, even more taking into account that this number also involves a high discharge rate of the battery.

Variant	Max. range	Max. endurance	Max. ascent rate	Hover rotor power
Reduced fuel storage	32.95 km	20 min	6 m/s	67.03 kW
Reduced maneuverability	255.02 km	2h 20min	2.5 m/s	77.38 kW

Table 4.12: Comparison of the actuations between the two-passenger variants considered.

Both alternatives can be defended and fitting applications can be found, of course. For instance, the reduced range version would still fit missions for short range urban commutes between concentrated points such as air taxis or medical emergencies. As for the second one, its range still allows it to perform trips between urban nuclei given that in those conditions the rate of ascent is not relevant. Another aspect to observe is that the alternatives presented could be replaced by a completely new conceptual model, preliminarily estimated at 900 kg and a required fuel cell power of 200 kW. While this model is not within the scope of the project, it is interesting to note that the resulting increase in payload does not follow a completely linear relationship given that the weight of all elements must increase in size and weight too. Fuel cells of this size are at this point possible

to manufacture and use for commercial vehicles but become harder to defend given their much higher current weight to power ratio.

A second variant of the one passenger model is to perform an adaptation in which the pilot is substituted by a remote control system, converting the aircraft into an UAV. Under these circumstances, the aircraft would be effectively over-dimensioned which in turn would give it additional capabilities such as enhanced range and endurance or higher maximum speeds. These actuations are summarized in *Table 4.13*.

		Cruise flight mode			
Parameter	**Cruise altitude**	**Maximum range**	**Maximum endurance**	**Maximum speed**	**Hover**
Rotor Power [kW]	0 m	54.74	40.02	82.83	56.86
	500 m	55.69	40.71	82.87	57.85
	1,000 m	57.71	42.19	82.93	59.91
Velocity [km/h]	0 m	143.57	60.99	199.90	0
	500 m	146.66	62.02	202.00	0
	1,000 m	150.69	63.38	202.80	0
Range [km]	0 m	363.76	215.78	310.24	0
	500 m	361.47	214.02	309.80	0
	1,000 m	352.33	208.81	307.23	0
Endurance [hr]	0 m	2.53	3.53	1.55	2.42
	500 m	2.46	3.45	1.53	2.35
	1,000 m	2.33	3.29	1.51	2.23

Table 4.13: Summary of actuations of the one-passenger model acting as a UAV.

At it can be observed, the range and endurance may be extended by up to 15% given the reduced payload. The maximum speed would also be increased, reaching values over 200 km/h, making this model very suitable for longer range emergency cargo transport among other applications. As for the ascent, the reduction in the weight allows for a much wider range of ascent rates and even altitudes, as shown by *Figure 4.15*. The battery becomes unnecessary until an ascent rate of $V_z = 7\ m/s$, something that would alleviate some of the pressure on the weakest aspect of this model.

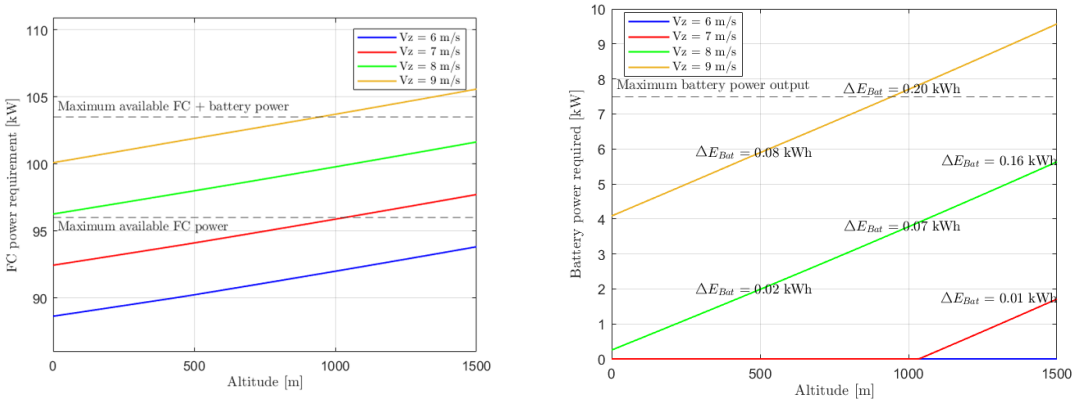

Figure 4.15: Evolution of the power consumed by the one-passenger remotely-controller vehicle as it ascends at different rates (left) and power required by the battery at each point (right), noting the battery energy consumption at the cruise mission altitude and at its double.

It is worth noting that, while useful as a thought experiment, if the model was to be implemented without a pilot, certainly part of the mass would be taken up by additional payload to make the trips economically viable. Therefore, it can be expected that related applications actually have actuations in between those shown in *Tables 4.11* and *4.13*.

4.4 Design balance

In order to conclude the adaptation, it is of interest for future related developments that some insight is given into the challenges that this technologies will most likely face in the following decade. With this purpose, the following section adds a summary of interesting remarks to be taken into account for the next steps necessary to develop this project or one similar.

4.4.1 Aerodynamic considerations

In order to optimize aerodynamic performance, focus needs to be put in two main areas: fuselage drag reduction and efficient rotor design.

Reducing the drag generated by the fuselage is essential to cut down parasitic power and thus reduce the overall power required to operate. To give some perspective, fuselage is estimated to contribute with 30-40% [33], [55] of the total parasitic drag, which applied to the previously presented results, represents between 4-5 kW of power the motor has to supply solely for this purpose. It is for this reason that new drag reduction methods are being currently studied, mainly within two approaches.

The first approach to reduce fuselage drag would focus in finding the optimal shapes and integration between components in order to generate directly more favourable conditions for flow adherence and the reduction in intensity of the generated vortices. This approach, commonly referred to as "passive drag reduction" has been very fruitful thanks to advanced CFD simulations. Among many particularities, it has been discovered that a circular cabin cross-section improves the overall behaviour of the aircraft at the wide range of angles of attack it operates [22], [53], keeping a nose shape such that the ratio of its radius to the fuselage width is lower than 0.1 [22]. Other characteristics are more common in the industry, such as avoiding sudden changes in curvature, elements that increase overall roughness such as rivets, holes, etc. or gradually decrease the aft fuselage cross section to avoid flow separation (area rule).

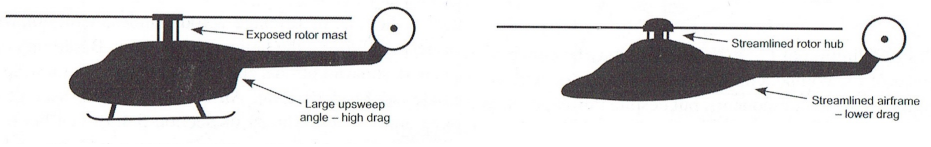

Figure 4.16: Example of fuselage designs with enhanced (right) and reduced (left) aerodynamic characteristics. Leishman [33].

Other findings, now related to the rest of the airframe components, show the benefits of smartly locating exterior components on the tail section in order to both reduce frontal area and keep the area rule [22]. This matter would precisely apply to the fuel tanks which in ideal conditions should be located in the interior of the aircraft or in a position where the drag increase generated is minimal. However, taking into account the size of this vehicle, either alternative seems unlikely unless an ideal reshaping of the interior allows for their introduction. In terms of reducing the impact of these devices while keeping them in the exterior, the simplest solution is to cover them with clean fairings, a measure that

has been proven effective before [45].

Alternative improvements are the introduction of "active drag reduction" mechanisms such as vortex generators or synthetic jet actuators, which show a promising potential in reducing the pressure gradient and thus the excess drag on the helicopter airframe [5], [14].

Other point of interest is the efficient choice stabilizer characteristics. For light helicopters, the stabilizers are often restricted to one side T-tail designs in order to optimize both weight and aerodynamic characteristics, given that forward mounted stabilizers require a heavier structure and aft-mounted low stabilizers have been proven to be very aerodynamically inefficient [33].

Regarding rotor design, the main challenges arise regarding the optimization of blade and airfoil design taking into account the complexity and coupling of aerodynamic phenomena of rotating systems. Generally, a reasonable combination of taper ratio at the tips and blade twist lead to reduced tip losses and thus a higher figure of merit [33]. Additionally, advanced tip design plays a big role in reducing profile losses. Figure 4.17 shows examples of state of the art designs for this purpose. Interesting studies such as those performed by Walsh et al. [61] and more recently by Vu et al. [59] have been focused on developing integrated blade optimizing methods for different rotor designs with very good experimental results.

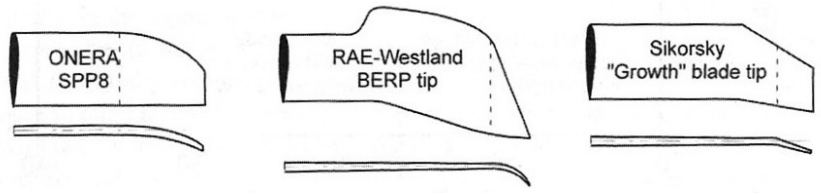

Figure 4.17: Advanced blade tip desgins. Source: Leishman [33]

The introduction of advanced airfoils in helicopter design is also set to increase efficiency, given that the airfoil chosen in the project was a first generation airfoil, design goals and recent developments are pushing the previous boundary and are expected to improve the figure of merit by 15%. However an empirically discovered limit has shown that practical values of $FM > 0.8$ are very hard to come by as a direct result of the disadvantages of low drag airfoil sections, such as lower maximum lift and higher pitching moments [13].

4.4.2 Propulsive considerations

Regarding the power generation of the helicopter, mainly the fuel cell and the electrical motors, several details should be considered.

Among them, one of the main concerns the model may cause is the introduction of two independent motors without a transmission system in order to reduce the overall weight of the model. This technique is, admittedly, not very common in the helicopter industry and may very well be substituted by a traditional transmission system and gearbox systems. As an example, take for instance the main rotor engine, an estimated 100

kW model that should induce a rotational speed of the blades of an estimated 530 rpm for the cruise altitude. If this was to be implemented as such, commercially available models would not fit the application since they are usually considered to be used with a reduction gearbox that adjusts the rotational speed to the corresponding conditions. Given that the scope of this project is merely quantitative and its desire is to propel future projects this discussion is not considered in the main design, but it is worth noting here that what is suggested effectively means that a specific design for the electric motor would be required to fit the conditions stated.

Additionally, placing a secondary motor at the tail, whose weight is estimated around 3 kg would affect the overall center of gravity of the aircraft as has been explored previously. Even if this is not a cause for concern right away, the logistics of powering that motor and locating it in a safe position should be considered. Solutions to the powering of the motor without the exposure of the cabling can begin by designing the tail boom so that it is able to contain the cables within, something whose study is out of the scope of this project. Regarding the exposure of the motor, the choice must consider that size is essential for the application, so smaller variants available for light aircraft or drones may very well suit this case and allow for simple casings or tail designs that protect the element.

For the fuel cell, the main design choice would be to select the type to be used given the wide range of options available. As introduced in *Chapter 3*, fuel cells are classified according to the electrolyte used, which in turn also characterizes the overall power output and optimal working conditions. *Table 4.14* summarizes the characteristics of the main types of fuel cell technologies. Generally, the most common types applicable for vehicle design are polymer electrolyte membrane (PEM) followed by alkaline (AFC). The reasoning for this is their quick start-up time and higher specific power and power density. However, exposure to impurities can reduce the effectiveness and lifetime of the fuel cells, which given that their cost is already high is not ideal.

Type	Electrolyte	Typical stack size	Applications	Advantages	Disadvantages
PEM	Perfluoro sulfuric acid	1 - 100 kW	Backup power, distributed generation, specialty vehicles, etc.	Corrosion resistance, low temperatures and quick start-up times	Expensive catalists and sensitive to impurities
AFC	Alkaline polymer membrane	1 - 100 kW	Military, space, back-up power, transportation, etc.	Low cost components, low temperature and quick start-up times	Sensitive to CO_2 and corrosion, higher volumes
PAFC	Phosphoric acid	5 - 400 kW (100 kW modules)	Distributed generation	Suitable for CHP and increased impurities tolerance	Expensive catalists, sulfur sensitivity and long start-up times
MCFC	Molten alkaline carbonates	300 kW - 3 MW (300 kW modules)	Electric utility, distributed generation, etc.	High efficiency, fuel flexibility and suitable for CHP	High temperature, corrosion sensitivity, low power density and long start-up time
SOFC	Ytria stabilized zirconia	1 kW - 2 MW	Electric utility, distributed generation, etc.	High efficiency, fuel flexibility, corrosion resistance and suitable for CHP	High temperature, corrosion sensitivity, limited number of shutdowns and long start-up time

Table 4.14: Summary of main fuel cell types characteristics. Source: U.S. Department of Energy [12].

The volume and location of the fuel cell will also be of particular interest given that, for instance, for the 120 kW fuel cell, the expected volume would be $0.185m^3$. Relative to the complete fuselage volume that result is approximately 7%, which is not a cause to worry as long as the overall equipment distribution is efficient.

4.4.3 Constructive and economic considerations

Regarding the material choice, it is increasingly clearer that the use of composite materials for the main structural elements of aircraft is a next-generation alternative that yields both high resistance-to-weight ratios as well as good vibrational performance. These characteristics are the perfect match for light helicopters given their need to reduce weight from all possible sources in order to increase the maximum payload. Additionally, fiber reinforced materials have the advantage of being able to be tailored in order to maximize mechanical properties according to their use by adjusting the fiber orientations and composition. Furthermore, the original model this project is based on already considered the construction of the cabin and rear structures as a mix of several widely-used composite materials such as Kevlar or carbon fibers given the technological trends and needs.

However, some of these materials tend to have poor impact resistance, which may lead to the introduction of metal reinforcements or impact reduction technologies that compensate these defects, given that the takeoff and landing cycles of helicopters can compromise the materials. Additionally, composite materials pose other challenges such as higher overall design complexities, costs and repair difficulties compared to their metal counterparts. More efficient manufacturing methods and the demand increase of these materials will eventually have a lower economical impact but maintenance capabilities will for now remain a challenge worth exploring given the industry needs.

In a similar fashion, the need to optimize the weight and volume of the different elements is a serious challenge for light helicopters and specially for air taxi applications. Take for instance the helicopter presented by the project: given the available cabin surface and including the areas required by two seats and the cabin controls, approximately 70% of the cabin floor area would already be occupied. The rest would be dedicated for the payload or additional elements that require being in the interior of the helicopter such as the fuel cell system. The efficient use of the available space of the aircraft while maintaining passenger comfort can be considered a limiting factor in the development of these models and should be further studied in deeper analysis.

An additional economic factor that should be interesting to consider is the current state of hydrogen distribution for aircraft. This point has already been discussed but, ideally, hydrogen should be produced at a near location, liquified and already available for refueling purpose at the corresponding aircraft storage site. However, current infrastructure is lacking of any of the three main components so for the sake of realism, it is unlikely that first iterations of the aircraft have available on-site production of fuel, which in turn would cause additional costs derived from transporting liquid hydrogen from centralized locations. Innovative projects such as *Picea* at a domestic level or *Hydrohub's* green hydrogen plant [1] at an industrial level, currently being developed are set to improve these conditions over time, and estimates say 2040 is a reasonable limit to have a well-formed infrastructure for general refueling purposes [2].

Chapter 5

Life cycle assessment

With this project focusing on the potential long term benefits of hydrogen propulsion, it is interesting to test the actual environmental impact of the designed models as a counterpart to their original design. The objective of this section will be to perform a so-called *cradle-to-grave* analysis focused around the total greenhouse gas (GHG) emissions of the models and discuss the current and future projection of hydrogen as a fuel for aviation.

5.1 Introduction

With the already presented environmental challenges facing worldwide populations and the increasing concern around fossil fuels, the movement towards increasing the share of renewable energies in the last decade has been noticeable. Hydrogen has also emerged with its corresponding interest and expectation as the ideal fuel source for the future: available, unlimited and clean. However, the truth is that there are very negative aspects of hydrogen holding it back from reigning supreme over the competence. For once, while hydrogen consumption is indeed absolutely neutral for the environment in terms of carbon emissions, it's current production is far from it.

There are, broadly speaking, two alternative ways of producing hydrogen: natural gas reforming and electrolysis. In the former, hydrogen is extracted from a hydrocarbon, usually methane, through thermo-chemical processes known as steam reforming and partial oxidation and generating as byproduct carbon dioxide. Hydrogen generated with this method is commonly called *grey hydrogen*. The procedure's impact can be reduced with the addition of a process known as carbon capture, generating a "cleaner"[1] fuel, usually denominated *blue hydrogen*. In contrast, hydrogen can also be generated through electrolysis, that is, extracting hydrogen gas from water molecules, generating no harmful waste. In the case the electricity required for the hydrogen generation comes from renewable sources, it is commonly referred to as *green hydrogen*. However, given the current available energy share, electrolysis is not be as "green" as one might think.

[1] While carbon capture has shown very clear emission reduction capabilities, life cycle studies show that current methods also influence in a negative way due to the required energy to carry them out, ending up with only a slight improvement (around 15%) [27].

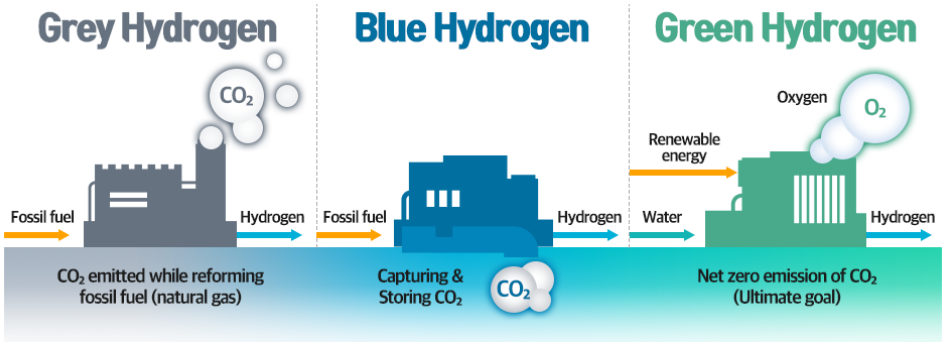

Figure 5.1: Summary of the main types of hydrogen according to their production process. Source: Gasunie [62].

In addition, problems related to transport and storage must also be mentioned, since in the current situation the most plausible proposal for hydrogen production is a centralized plant which needs a distribution infrastructure that has been proven very inefficient both in terms of energy losses (pipelines) and environmental impact (land transportation to refueling stations). Once hydrogen reaches its commercial distribution site, energy must be used to maintain the temperature in the case of liquid hydrogen. Combining all of this problems has inadvertently surrounded hydrogen with a smoke of criticism and doubt, sometimes going as far as labelling it a failure partly due to the unreasonable expectations around it.

Far from getting carried away with any of these tendencies, this project is focused in an objective analysis of the current impact of fuel cell-powered vehicles like the ones conceptualized in previous chapters. The tool used to perform this analysis is a life-cycle assesment or LCA, a widespread methodology used to evaluate the environmental impacts of products or activities during their lifetimes. Dating back to the early 1970s, the analysis became standardized in 2006 through the norm *ISO 14040:2006* [19] with the objective of facilitating data exchanges and a more robust consensus around the procedures. This robustness is primordial to prevent the spread of misinformation around a critical topic like environmental impact.

Many types of studies can be performed using this methodology, but the study will be focused on GHG emissions, evaluating the contribution of the model from its production to its disposal in terms of equivalent kilograms of carbon dioxide.

5.2 Methodology and limitations

A cradle-to-grave analysis for a given transport technology should include the impact of the differentiated stages in the vehicle's life: fuel production (*well-to-tank*), vehicle production (*cradle-to-gate*) and operation cycles (*tank-to-wheel*). In this case the analysis will be performed over the original ICE-powered helicopter and the adapted one-passenger hydrogen fuel cell-powered model developed in the project. In order to strictly follow LCA guidelines [29], the following aspects must be defined first:

System boundaries

Defined as the activities contributing to the environmental consequences, which in this case specifically referred to the raw materials used and the energy mix (both for 2020 and the expected for 2030) in terms of system inputs, while wastes in the form of atmospheric emissions as outputs. These system boundaries are reflected in *Figure 5.2*

Functional units

Next, it is essential to have a quantified description that the product to be analyzed fulfills. In terms of fuel production, the kilowatt-hour (kWh) in the form of the LHV of each fuel was used given their different physical and chemical properties. As for the vehicle production and operation, it was considered a total of 7,500 hours as as an estimated common life for the vehicle[2]. This number comes from an assumed mission fitting for both models' actuations further explained in the operation cycle description, expressed in terms of hours as it is, in this case, a more representative quantity of the vehicle operation. Emissions will therefore be expressed for the production and operation of one vehicle according to this lifetime estimation.

Impact category

This term refers to sets of environmental issues to which the results of the study may be assigned. Among the several categories commonly considered for LCAs, global warming was the one chosen for the study given it is currently the most important environmental concern. To do so, CO_2, CH_4 and NO_2 emissions were considered accounting for their different global warming potential (1, 23 and 296 respectively). Thus, in order to carry out the calculations the range of GHG emissions were expressed in terms on equivalent kilograms of CO_2.

Life cycle inventory

The origin of the data used for the analysis was taken predominantly from the GREET® v2021 and GaBi databases.

More specifically, the energy mixes[3] were obtained using the GaBi database. Two scenarios were considered, Europe 2020 and Europe 2030, with the objective of projecting the study into the next decade. The different energy mixes were firstly used to obtain the estimated fuel production emissions for the different types of hydrogen and for gasoline, shown in *Table 5.1.*

The estimated energy mix results were also fed as input to GREET® v2021, where data referred for raw and intermediate materials making up the structure and components of the aircraft as well as fuel production data were obtained. Note that some components such as hydrogen tanks, transmission systems or landing gears were calculated from their estimated material composition while manufacturing data for fuel cells, batteries, electrical motors and internal combustion engines was already available. Alternatively, data concerning the manufacturing of electrical motors and batteries was calculated with GaBi.

[2]Note that this value does not imply specific life span calculations for the given production and operation cycles but rather, frames a realistic value at which the operational life of the vehicles could be evaluated without compromising the results' relevance.

[3]Primary sources distribution from which usable energy like electricity is obtained.

	Production emissions $[kWh]$	
	2020 energy mix	**2030 energy mix**
Grey hydrogen	0.419	0.385
Blue hydrogen	0.217	0.180
Green hydrogen	0.132	0.098
Gasoline	0.078	0.071

Table 5.1: Fuel production emission comparison.

The composition specified for the different elements included in the corresponding vehicle models is summarized in *Table 5.2*, except for the more complex compositions which were omitted for clarity. Note that electronic elements such as avionics, power electronics or instrumentation were not considered in the study given their specificity and mission dependence.

	Composition		Mass [kg]	
Element	**% in weight**	**Material**	**Original**	**H_2 adaptation**
Fuselage	80 % 20 %	Carbon fiber Alluminium 2xxx	73.08	65.42
Tail structure	100 %	Carbon fiber	6.35	6.35
Landing gear	100 %	Alluminium 7xxx	6.50	6.50
H_2 tank	80 % 20 %	Alluminium 2xxx Polymer insulator foam	-	45.00
Gasoline tank	100 %	Stainless steel	6.50	-
Transmission system	100 %	Specialty steel		25.00
Rotor blades	70 % 30 %	Alluminium 7xxx Arbon fiber	50.74	47.11
Rotor hub	80 % 20 %	Mild steel Alluminium 2xxx	24.62	23.64
Miscellaneous supports	100 %	Alluminium 2xxx	10.00	10.00
ICE powertrain	GREET® v2021 database		78.00	-
H_2 fuel cell	GREET® v2021 database		-	184.18
Electric motor	GaBi database		-	64.21
Battery	GaBi database		10.42	10.42

Table 5.2: Element composition used to perform the vehicle production cycle analysis.

Life cycle characteristics

Finally, details for the specific parts of the life cycle evaluated must be provided to complete the full methodology picture. For the fuel production, the most important intermediate processes were considered: from the raw material extraction to the distribution of the final product, including additional factors such as raw material transportation. It is particularly interesting to analyze different production scenarios for hydrogen, starting from the current situation (estimated 97% *grey hydrogen* [2]) into future projections in order to compare the effects of the fuel origin on the environmental impact, using according energy mixes to complete their definition. Additionally, centralized fuel distribution was considered for both gasoline and hydrogen as it is the most realistic scenario for its distribution in the time span concerning the study.

For the vehicle production cycle, the emissions were calculated based on the raw materials required for each of the considered elements of the aircraft. The choice of materi-

als, summarized above, was based on the original model structural composition suggested by Tejada [56], GREET® and GaBi's material distribution for the corresponding aircraft elements and other references for the hydrogen tanks [64], gasoline tanks and transmission systems [17].

The aircraft operation cycle was defined with the objective of having a realistic scenario fitting for both the original and the one-passenger hydrogen-powered models' actuations. With this in mind, the mission was defined as 2 hours of operation per day with a total 30 minutes of hover, five times a week, at an intermediate velocity between maximum range and maximum endurance flight modes and at the design cruise altitude. This mission specification could fit both models as it can be descriptive from cargo transport to civil safety and emergency missions. Elongated for a period of time of approximately 15 years results in the functional unit previously defined for the vehicle operation. Additionally, refuelling efficiency for both models was assumed to be 100 %.

Finally, the vehicle disposal and recycling cycle was not considered in the study for several reasons among which stand-outs are the lack of aircraft recycling information and relevance in terms of the impact category being studied. The overall LCA methodology can be observed in *Figure 5.2*.

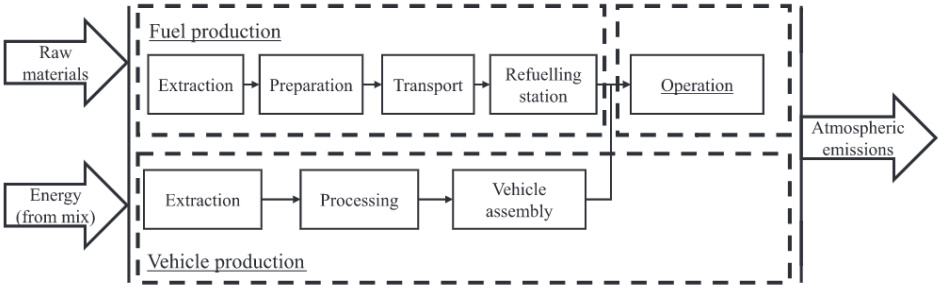

Figure 5.2: Life cycle assessment methodology, with the defined boundaries. Source: Desantes et al. [15]

As a final note before the results presentation and discussion, it is worth mentioning the limitations the study is subjected to, primarily in terms of data but also in its specificity. This is why the results to be presented must be considered within the constraints of the two specific models subject to the study up to this point and in the temporal span presented. The materials described in *Table 5.2* are based on preliminary design parameters and represent only a simplified version of the model, which may induce errors if performed after the model is conceived in detail. Additionally, the data used in the projected scenarios may very well vary as time passes, changing the conclusions reached with this study. Finally, recycling and disposal alongside other possible factors that were not yet accounted for may have an underestimated influence on the results.

5.3 Results and discussion

Starting with the vehicle production cycle, the results are segmented according to the main components of the aircraft in *Figure 5.3*. The final result indicates that the production of the original model represents, under the current energy mix, a total of 2396.7 $kg\ CO_2\ eq.$ while the adapted version surpasses this amount, reaching 3343.5 $kg\ CO_2\ eq.$ This means approximately a 50% increase, mainly due to the production of the fuel cell, which by itself causes 842.5 $kg\ CO_2\ eq.$ and, in a lower level, the fuel tanks. Another factor causing the increase in production emissions is that, given both aircraft are dimensioned for different MTOW, the estimated structural mass of the adaptation is slightly higher.

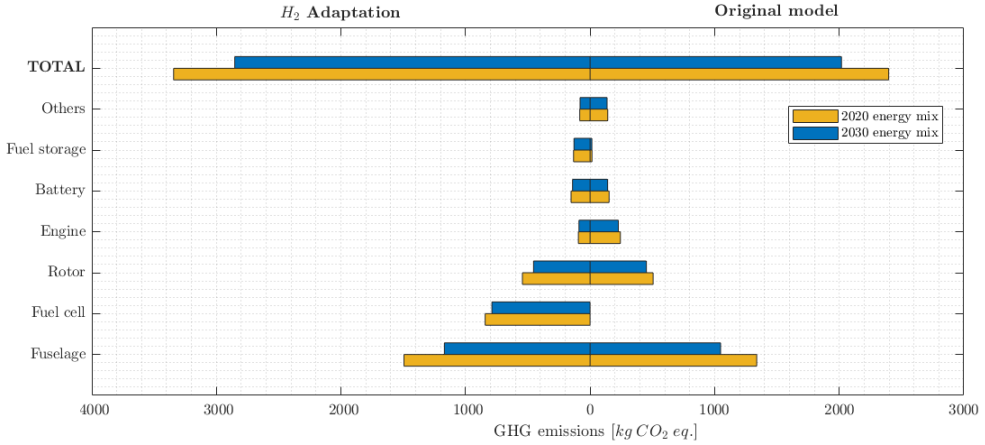

Figure 5.3: Results in terms of GHG emissions for the vehicle production cycle.

The estimation of next decade's energy mix does not close this gap but it reduces the impact of both models by 20% in the case of the conventional model and 17% for the hydrogen adaptation. This reduction is mainly due to the foreseen improvements in carbon fiber production and the increase in the share of renewable energies to power the processes needed to obtain the materials. Even with the removal of the transmission system and having electric motors which cost only a third in terms of emissions compared to the ICE, there is no denying the production impact of the adapted model is far worse than the original.

However, the vehicle production is only a small sample of the complete analysis. For the fuel production, several scenarios were assesed: first using the current energy mix and estimated distribution of hydrogen production [57], [58] and secondly, assessing two future prospects with next decade's energy mix. These prospects differ on the optimism towards the conversion into *green hydrogen* expected following the European "Hydrogen road-map"" [2], where the predicted hydrogen production is compared between an SMR-dominant and an electrolysis-dominant scenario.

As it can be observed through *Figure 5.4*, the difference between scenarios is slightly affected, having at most a 25% overall reduction in the hydrogen production, but more concerning is the clear overall difference between hydrogen and gasoline (whose emissions are practically not affected by the changes in the energy mix).

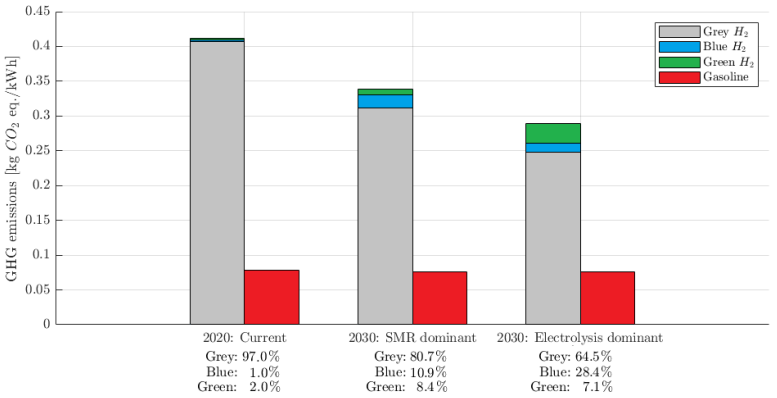

Figure 5.4: GHG emissions per kWh of hydrogen and gasoline under the different scenarios considered.

Hydrogen's impact in terms of GHG emissions is considerably higher than gasoline's regardless of the production method considered in these energy mixes, as shown in *Table 5.1*. In general, the only comparable production method is electrolysis, but even then its impact is almost double that of average gasoline production. Going even further, it is notable how, even for reduced grey hydrogen scenarios, its effects are very notable, as its production is five times more negative than gasoline and more than double of their hydrogen counterparts.

The total fuel required can be calculated through the breakdown of energies used for each case, taking into account the weight differences, summarized in *Table 5.3*. Note that the takeoff (5 m/s) and landing (2 m/s) were considered in the calculations additional to the actual cruise time. In terms of fuel efficiency, for the fuel cell the same data as that used along *Chapter 4* was used, while for the ICE a 35% fuel efficiency will be considered as a best-case scenario [4].

	Net energy required $[kWh]$				**Fuel energy (including fuel efficiency)** $[kWh]$				
Aircraft	**Takeoff**	**Cruise**	**Hover**	**Landing**	**Takeoff**	**Cruise**	**Hover**	**Landing**	**TOTAL**
Adapted model	2.43	72.97	34.65	3.63	5.38	128.88	61.19	6.51	201.96
Original model	1.71	51.64	22.54	3.09	4.88	147.54	64.40	8.83	225.65

Table 5.3: Energy consumption for each part of one mission cycle (2 h), attending to the described fuel efficiencies.

As it can be observed, in principle the required energy would be higher in the case of the FCV, but given the improved propulsion system efficiency, the total required energy (fuel energy) is lower and thus, a lower amount of fuel needs to be produced. This is an interesting result, since it shows that long term usage of optimized fuel cells can lead to reduced fuel production costs and environmental impact under the right circumstances.

The operation cycle is analyzed following the previously described mission. Note that in the case of hydrogen, no GHG emissions are caused in terms of operation, while for the Rotax-914, using gasoline the number is 8.87 $kg\,CO_2/gal$ [23]. The specific fuel consumption of the engine for these conditions is approximately 4.8 gal/h [49] so, over the total lifetime considered the total emissions of the gasoline-powered vehicle are 319,932 $kg\,CO_2\,eq$.

Finally, comparing the overall *cradle-to-grave* cycle shows that the emissions saved during the operation phase are able to outweigh the disadvantages in the vehicle and fuel production cycles. The results are shown for the different scenarios in *Figure 5.5*.

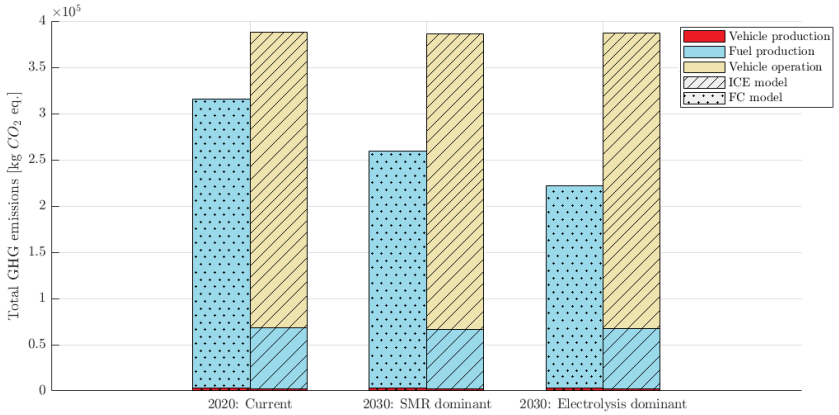

Figure 5.5: Total emissions of the considered models for the different scenarios in the defined *cradle-to-grave* analysis.

As it can be observed, even with the current hydrogen distribution and energy mix, the results are favorable for the hydrogen adaptation, resulting in an overall decrease in emissions of 18.75% (approximately 73,000 $kg\,CO_2\,eq$). As for the Europe 2030 mix scenario, the results show that emissions could be reduced by 32.08% in the case of the SMR-dominant case to 42.48% in the case of an electrolysis dominant case. Note that after the study, compared to the that of the other cycles, the vehicle production impact is negligible (less than 1% across all scenarios).

This is clearly due to the elevated operational impact of the original model with respect to the adaptation. There is an argument to be made that a shorter life-time vehicles, the usage of fuel cells may not be as positive given their higher fuel production emissions. However, very similar results are found for a very wide range of operational lifetimes, which is explainable given that the combination of fuel production and vehicle operation emissions, which are of course related for a given mission, is between 18 and 42 % lower in favour of fuel cells.

It is clear though that, while the results clearly benefit the hydrogen adaptation, there is still much room to improve given that almost all of the carbon footprint of the fuel cell vehicle is caused by the hydrogen production. This suggest that, if the objective is to further reduce GHG emission, the share of renewable energies and H_2 production via electrolysis must increase considerably in the next decades. This decision, however, is not only of environmental relevance as it is not a secret how green hydrogen production is much more expensive in the short term than the other alternatives. Increasing the efficiency and reducing the costs of electrolysis must therefore be a clear future goal in order to promote funding on renewable energy research and production. Improvements on these areas would allow green hydrogen to become economically advantageous in the long term given it relies on cheap renewable energies, which are benefited from large scales.

Chapter 6

Conclusion and future steps

Once the whole project has been developed, it is important to reflect back on its objectives, methodology and results, and discuss the main ideas that have been extracted and their relevance, taking into account the own limitations of the study. Additionally, given the nature of this topic, the next steps towards the actual model implementation must be discussed and contextualized.

6.1 Conclusion

Along this project, the implementation of a hydrogen fuel cell as the powerplant of a light helicopter was performed making use of a previously calculated model. The main objective of the adaptation was to conceptualize an aircraft capable of responding today's transport problems, specially those related with environmental impact and traffic congestion. The relevance of the study was first assesed in a brief market analysis in which the market niche for this type of aircraft was found to be growing at a rapid rate given their use in civil safety, emergency and agricultural missions. Furthermore, with the development of the so-called *air taxis*, the window of opportunity is wide open for vehicles like the one developed, which not only are favored in terms of flexibility but also as a way to move towards cleaner and more sustainable means of transportation.

After the introduction of a brief theoretical background on aerodynamic calculations for helicopters and hydrogen fuel-cells operation and performance, the methodology followed to complete the study was presented. The proposed procedure consisted in an iterative dimensioning of the structural and power elements of the aircraft for a specific mission through statistical relationships and aerodynamic requirement calculations. This methodology was implemented through MATLAB®, accelerating the calculation time and allowing for different variants to be analyzed, further exploring the applications and advantages, as well as narrowing down the limitations of fuel-cell powered aircraft. The different considered variants of the adapted model consisted in an UAV, a one-passenger aircraft and two modifications of the latter, exploring its performance operating driver-less or with one extra passenger.

In terms of aircraft dimensions, the UAV model was estimated at a design mass of 415.72 kg, requiring a fuel cell with a nominal power of 80 kW, while the one-passenger aircraft reached 608.38 kg, requiring in this case a 120 kW fuel cell. The performance of these aircraft was analyzed using performance data of fuel-cells obtained through state of the art dynamical simulations in the specified altitude range. Interestingly, it was found that even when the adapted version was heavier, the actual fuel required to performed the designed mission was reduced thanks to the improved efficiency of the powerplant. Even then, it is important that, for future iterations of fuel cell helicopter designs, the specific power of the fuel cell is increased, while the gravimmetric density of the hydrogen tanks is decreased, since they were two of the main sources of mass increase.

The conclusions reached through the study of the different aircraft actuations is that not only their applicability is currently possible, but they are competitive in terms of range, endurance and maneuvering with similar aircraft, having additional benefits compared to their conventional ICE counterparts such as their reduced environmental impact. These environmental benefits were further explored in a comparative *cradle-to grave* analysis between the original aircraft and the adapted version, using the chance to discuss the current state of the art in hydrogen economy. Trough a LCA methodology focused on global warming through the analysis of GHG emissions, the study found that if implemented today, the adapted model could reduce the overall impact by 18%. Furthermore, the case was explored in two future Europe 2030 scenarios where hydrogen production settles either on SMR or electrolysis. In this case, the impact level of the adapted aircraft improved by 32% and 43% respectively, showing the importance of an environmental policy focused on sustainability and the increase in renewable energy usage.

It is critical to also assess the limitations of the project, beginning by the lack of specific bibliography related to light helicopters, a factor that may affect both the performed structural mass and the aerodynamic performance calculations given they made use of preliminary design models for general helicopter applications. Additionally, specific aerodynamic parameters such as the parasitic drag coefficient of the aircraft were not studied in depth as they did not belong to the scope of the project but instead were found from statistical correlations, which may have an impact on the presented results. As for the methodology, both in the case of the adaptation of the model and the environmental impact analysis, a series of simplifying hypothesis were made trying to always have a consistent criteria, which should be taken into consideration before rushing into the usage of the results. Other sources of error or criticisms related to the methodology should be taken into consideration given the academic nature of the project and the limited resources available.

Considering the outcome and the presented sources of error, the results and conclusions obtained throughout the project's development are considered relevant in the current context of the aerospace sector, as a fuel-cell powered light helicopter was proven to be a competitive vehicle for future mobility, cargo transport and civil safety. The objectives proposed in the first pages were therefore met successfully, reaching clear and objective conclusions through a well-defined methodology, always considering a certain safety margin in order to account for possible design changes and unexpected factors that may affect the overall performance of the designed aircraft. In terms of additional value presented by the study, a simple preliminary design software was developed for fuel-cell powered helicopter applications which, while very specific in terms of usage, is very convenient and has shown good results during the study development.

6.2 Future steps

The presented study only assesses preliminary design aspects of the vehicle, representing a basis for the continuation with more in-depth analysis of its individual aspects. The list of possible studies to be performed after this project's results is endless and each one very important in its own right. Some of the most relevant in order to continue with the design cycle are:

- Achieving a higher level of detail in the preliminary 3D design taking into consideration the recommendations presented in this project according to the state of the art.
- Using the aforementioned design in order to more accurately estimate the masses of the different elements and have a more strict criteria on the material selection.
- Performing detailed aerodynamic calculations of individual aspects of the aircraft, mainly fuselage drag, rotor efficiency and non ideal effects, element interference and blade profile design. This study is key since some of the data used during this project is originated from statistical relationships, not specific study results.
- In a similar manner, perform specific structural studies focusing specially on the aircraft overall resistance and durability, as well as its behaviour during critical maneuvers such as landing or hovering. Specially interesting is the study of the vibrational characteristics of the aircraft in order to optimize comfort, reduce the noise impact and avoid dangerous phenomena such as ground resonance.
- Obtaining simulations on the aircraft flight dynamics in order to predict undesired behaviours and correct them during the design phase. As for the UAV, these results could be used to develop the required software to either remotely control the aircraft or implement an automatic pilot able to perform the assigned missions.
- Developing efficient control systems that allow for the correct and pleasant maneuvering of the aircraft, specially considering its potential private use.
- Adapting the interior space of the aircraft according to the mission and efficiently distributing the different elements, which in turn can suggest if the aircraft is in need of an overall resizing.

As for hydrogen usage in aviation, many challenges are still to be faced and even discovered. As it has already been discussed the lack of infrastructure is the most immediate problem preventing hydrogen vehicles to continue developing. For that reason it is key to continue with the development of different initiatives related to all areas of hydrogen economy: from fuel production to vehicle operation, there is room for improvement across all fields and future studies should aim to continue with the momentum generated in the last decade. Finally, it is also key to develop environmental policies focused on the increase in renewable energy production and usage, helping to move the hydrogen production into a more electrolysis-dominant market, where the environmental benefits have been proven optimal.

Bibliography

[1] "A one-gigawatt green-hydrogen plant advanced design and total installed-capital costs," Hydrohub Innovation Program, 2022. [Online]. Available: https://ispt.eu/gigawattscale/.

[2] "A sustainbale pathway for the european energy transition. the hydrogen roadpmap.," *Publications Office of the European Union*, 2019. DOI: 10.2843/249013.

[3] "Air taxi market is expected to reach $6.63 billion by 2030," Allied Market Research, 2021.

[4] A. Albatayneh, M. Assaf, D. Alterman, and M. Jaradat, "Comparison of the overall energy efficiency for internal combustion engine vehicles and electric vehicles," *Environmental and Climate Technologies*, vol. 24, pp. 669–680, Oct. 2020. DOI: 10.2478/rtuect-2020-00.

[5] B. G. Allan and N. W.Schaeffler, "Numerical investigation of rotorcraft fuselage drag reduction using active flow control," NASA Langley Research Center, 2011.

[6] A. Bharti and R. Natarajan, "Chapter 7 - proton exchange membrane testing and diagnostics," in *PEM Fuel Cells*, G. Kaur, Ed., Elsevier, 2022, pp. 137–171, ISBN: 978-0-12-823708-3. DOI: https://doi.org/10.1016/B978-0-12-823708-3.00007-9. [Online]. Available: https://www.sciencedirect.com/science/article/pii/B9780128237083000079.

[7] R. M. Carlson, "Helicopter performance—transportation's latest chromosome: The 21st annual alexander a. nikolsky lecture," *Journal of the American Helicopter Society*, vol. 47, 1 2002.

[8] A. Carter and J. Darland, "Supernal and urban-air port debut world's first functional advanced air mobility vertiport," *Supernal*, Apr. 2022.

[9] "Clean sky 2," Clean Sky Joint Undertaking, 2015.

[10] "Commercial helicopters global market report," Business Research Company, 2022.

[11] "Commercial helicopters market overview," Mordor Intelligence, 2021.

[12] "Comparison of fuel cell technologies.," U.S. Department of Energy. [Online]. Available: https://www.energy.gov/eere/https://www.energy.gov/eere/fuelcells/comparison-fuel-cell-technologies.

[13] Á. Cuerva Tejero, J. L. Espino Granado, Ó. López García, J. Meseguer Ruiz, and Á. Sanz Andrés, *Teoría de los helicópteros*, 2nd ed. Garceta, 2012.

[14] F. De Gregorio, "Helicopter fuselage model drag reduction by active flow control systems," Sep. 2017.

[15] J. M. Desantes, R. Novella, L. M. García-Cuevas, and M. Lopez-Juarez, "Feasibility study of a fuel-cell powered unmanned aerial vehicle with 75 kg of payload," 2021.

[16] "Doe technical targets for fuel cell systems and stacks for transportation applications," U.S. Department of Energy. [Online]. Available: https://www.energy.gov/eere/fuelcells/doe-technical-targets-fuel-cell-systems-and-stacks-transportation-applications.

[17] R. Drago, "Endurance and failure characteristics of modified vasco x-2, cbs 600 and aisi 9310 spur gears," 1981.

[18] P. A. Eisenstein, "Uber has offloaded its elevate unit, but flying taxis are still taking off," 2020. [Online]. Available: https://www.nbcnews.com/business/autos/uber-has-offloaded-its-elevate-unit-flying-taxis-are-still-n1250863.

[19] "Environmental management — life cycle assessment — principles and framework," International Standard Organization, 2006.

[20] M. Escudero-Escribano, "Electrocatalysis and surface nanostructuring: Atomic ensemble effects and non-covalent interactions.," 2011.

[21] J. I. Giménez-Nadal, J. A. Molina, and J. Velilla, "Trends in commuting time of european workers: A cross-country analysis," *Transport Policy*, vol. 116, pp. 327–342, Feb. 2022, ISSN: 1879310X. DOI: 10.1016/j.tranpol.2021.12.016.

[22] G. A. da Graça Pereira, "Drag reduction of airframe and non-lifting rotatory systems," University of Breda Interior, 2009.

[23] "Greenhouse gases equivalencies calculator - calculations and references," United States Environmental Protection Agency, 2022. [Online]. Available: https://www.epa.gov/energy/greenhouse-gases-equivalencies-calculator-calculations-and-references.

[24] *Healthy environment, healthy lives how the environment influences health and well-being in Europe*. 2019, ISBN: 9789294802125.

[25] "Helicopter market size," G. M. Insights, 2022.

[26] "Helicopter market size, share covid-19 impact analysis," 2021.

[27] R. W. Howarth and M. Z. Jacobson, "How green is blue hydrogen," *Energy Science Engineering*, vol. 9, pp. 1676–1687, 10 Aug. 2021.

[28] D. Howell, B. Cunningham, T. Duong, and P. Faguy, "Overview of the doe vto advanced battery rd program david howell (presenter) brian cunningham tien duong p," U.S. Department of Energy, 2016.

[29] A. A. Jensen, L. Hoffman, B. T. Møller, and A. Schmidt, "Life cycle assessment (lca): A guide to approaches, experiences and information sources," *Environmental Issues Series*, 6 2014.

[30] Y. Jiang, L. Kang, and Y. Liu, "Optimal matches with load shifting strategy in hybrid power system considering varied price of outsourced electricity," *13th International Symposium on Process Systems Engineering (PSE 2018)*, Computer Aided Chemical Engineering, vol. 44, M. R. Eden, M. G. Ierapetritou, and G. P. Towler, Eds., pp. 1057–1062, 2018, ISSN: 1570-7946. DOI: https://doi.org/10.1016/B978-0-444-64241-7.50171-3. [Online]. Available: https://www.sciencedirect.com/science/article/pii/B9780444642417501713.

[31] W. Johnson, *Helicopter Theory*. Dover Publications INC., 1994, ISBN: 978-0-486-68230-3.

[32] M. Langfield, "Getting a clear picture: Procuring the right surveillance equipment for police aviation," *AirMed Rescue*, Jul. 2021.

[33] J. G. Leishman, *Principles of Helicopter Aerodynamics*, 6th ed. Cambridge University Press, 2006.

[34] R. Lemos, "The helicopter: A hundred years of hovering," 2007. [Online]. Available: https://www.wired.com/2007/12/gallery-helicopter/.

[35] "Light helicopter," 2017. [Online]. Available: https://grabcad.com/library/light-helicopter-1.

[36] J. L. López-Ruíz, *Helicópteros: teoría y diseño conceptual.* Universidad Politécnica de Madrid, 1993.

[37] A. Madhukalya, "Ola announces electric flying car airpro, but there's a catch," 2021. [Online]. Available: https://www.businesstoday.in/latest/trends/story/ola-announces-electric-flying-car-airpro-but-theres-a-catch-292342-2021-04-01.

[38] G. Martin, "Toyota invests $394 million in electric air taxi company joby aviation," *Forbes*, Jan. 2018. [Online]. Available: https://www.forbes.com/sites/grantmartin/2020/01/18/toyota-invests-590-million-in-electric-air-taxi-company-joby-aviation/?sh=468894b38ea0.

[39] S. Molina, R. Novella, B. Pla, and M. Lopez-Juarez, "Optimization and sizing of a fuel cell range extender vehicle for passenger car applications in driving cycle conditions," *Applied Energy*, vol. 285, p. 116 469, 2021, ISSN: 0306-2619. DOI: https://doi.org/10.1016/j.apenergy.2021.116469. [Online]. Available: https://www.sciencedirect.com/science/article/pii/S0306261921000349.

[40] M. Olszewski and S. A. Rogers, "Evaluation of the 2010 toyota prius synergy drive system," Oak Ridge National Laboratory Energy Efficiency and Renewable Energy, 2011. [Online]. Available: http://www.osti.gov/contact.html.

[41] E. Özbek, G. Yalin, S. Ekici, and T. H. Karakoc, "Evaluation of design methodology, limitations, and iterations of a hydrogen fuelled hybrid fuel cell mini uav," *Energy*, vol. 213, p. 118 757, 2020, ISSN: 0360-5442. DOI: https://doi.org/10.1016/j.energy.2020.118757. [Online]. Available: https://www.sciencedirect.com/science/article/pii/S0360544220318648.

[42] R. W. Prouty, *Helicopter performance, stability and control.* 3rd ed. Krieger Drive, 1995.

[43] S. Rajendran and S. Srinivas, "Air taxi service for urban mobility: A critical review of recent developments, future challenges, and opportunities," *Transportation Research Part E: Logistics and Transportation Review*, vol. 143, Nov. 2020, ISSN: 13665545. DOI: 10.1016/j.tre.2020.102090.

[44] R. Rapier, "Estimating the carbon footprint of hydrogen production," 2020. [Online]. Available: https://www.forbes.com/sites/rrapier/2020/06/06/estimating-the-carbon-footprint-of-hydrogen-production/?sh=4099509824bd.

[45] T. Renaud, A. Le Pape, and S. Péron, "Numerical analysis of hub and fuselage drag breakdown of a helicopter configuration," *CEAS Aeronautical Journal*, vol. 4, pp. 409–419, 4 Dec. 2013, ISSN: 18695590.

[46] J. J. Romm, "The hype about hydrogen," *Issues: Science and Technology*, vol. 20, 3 2004.

[47] J. Roskam, *Helicopter Theory*. DAR Corporation., 1985.

[48] C. Rotaru and M. Todorov, *Helicopter Flight Physics*. Feb. 2018, ISBN: 978-953-51-3807-5. DOI: 10.5772/intechopen.71516.

[49] "Rotax 912, rotax 912 uls, rotax 914 aircraft, engine fuel and torque specifications data," Ultralight News.

[50] M. Ruiz, "Air taxi market could reach 4 trillion dollars by 2035, says wisk ceo.," Feb. 2022.

[51] J. A. Sanguesa, V. Torres-Sanz, P. Garrido, F. J. Martinez, and J. M. Marquez-Barja, "A review on electric vehicles: Technologies and challenges.," *Smart Cities*, vol. 1, 4 2021.

[52] R. Shevell, *Fundamentals of Flight*. Pearson, 1988.

[53] W. Shi, J. Li, H. Gao, H. Zhang, Z. Yang, and Y. Jiang, "Numerical investigations on drag reduction of a civil light helicopter fuselage," *Aerospace Science and Technology*, vol. 106, p. 106 104, 2020, ISSN: 1270-9638. DOI: https://doi.org/10.1016/j.ast.2020.106104. [Online]. Available: https://www.sciencedirect.com/science/article/pii/S1270963820307860.

[54] "Source resistance: The efficiency killer in dc-dc converter circuits," Maxim Integrated, 2004.

[55] R. Stepanov, V. Zherekhov, V. Pakhov, *et al.*, "Experimental study of helicopter fuselage drag," 2016.

[56] P. Tejada Cánovas, "Diseño conceptual de un *light helicopter* para trabajos aéreos," Universidad Politécnica de Valencia, 2020.

[57] "The future of hydrogen," International Energy Agency, 2019.

[58] R. Thomson, U. Weichenhain, N. Sachdeva, *et al.*, "Hydrogen: A future fuel for aviation?" Roland Berger, 2020.

[59] N. A. Vu, J. W. Lee, and J. I. Shu, "Aerodynamic design optimization of helicopter rotor blades including airfoil shape for hover performance," *Chinese Journal of Aeronautics*, vol. 26, no. 1, pp. 1–8, 2013, ISSN: 1000-9361. DOI: https://doi.org/10.1016/j.cja.2012.12.008. [Online]. Available: https://www.sciencedirect.com/science/article/pii/S1000936112000167.

[60] S. C. Walpole, D. Prieto-Merino, P. Edwards, J. Cleland, G. Stevens, and I. Roberts, "The weight of nations: An estimation of adult human biomass," 12 2012.

[61] J. Walsh, W. LaMarsh, and H. Adelman, "Fully integrated aerodynamic/dynamic optimization of helicopter rotor blades," *Mathematical and Computer Modelling*, vol. 18, no. 3, pp. 53–72, 1993, ISSN: 0895-7177. DOI: https://doi.org/10.1016/0895-7177(93)90104-7. [Online]. Available: https://www.sciencedirect.com/science/article/pii/0895717793901047.

[62] "What is hydrogen?," [Online]. Available: https://www.gasunie.nl/en/expertise/hydrogen/what-is-hydrogen.

[63] F. M. White and G. H. Christoph, "A simple theory for the two-dimensional compressible turbulent boundary layer," *Journal of Basic Engineering*, vol. 94, pp. 636–642, 1972.

[64] C. Winnefeld, T. Kadyk, B. Bensmann, U. Krewer, and R. Hanke-Rauschenbach, "Modelling and designing cryogenic hydrogen tanks for future aircraft applications," *Energies*, vol. 11, 1 Jan. 2018, ISSN: 19961073. DOI: 10.3390/en11010105.

[65] M. Woods, "Government partners with wisk for world-first trial of self-flying air taxi 'cora' in canterbury," *Beehive*, Feb. 2020.

[66] G. Zorpette and E. Ackerman, "Evtol companies are worth billions—who are the key players?" *IEEE Spectrum*, Feb. 2022.

Appendix A

Budget

The following budget has been estimated according to the human and material resources needed to carry out the described project. Given its academic nature, most of the costs are related to the necessary software licenses to perform the required calculations and designs, as well as the time spent by the student, acting as a technical engineer. For this reason, it is considered, given the time span and the time dedicated to the project.

Note that the unitary prices mentioned are estimated according to the current date, June 2022, and may be susceptible to change for future calculations.

Quantity	Concept	Unitary price	Cost
30	**Hours of supervision and guidance by Doctor Engineer**	**40 €**	**1,200.00 €**
30	**Hours of supervision and guidance by Junior Engineer**	**20 €**	**600.00 €**
300	**Hours of project development by Technical Engineer**	**15 €**	**4,500.00 €**
80	Hours dedicated to documentation and formation		
100	Results extraction in *MATLAB*®		
20	Results extraction in *Micrsosoft Excel*®		
20	Analysis and validation of the results		
25	Results post-processing in *MATLAB*®		
5	CAD adaptation and ellaboration of blueprints in *AutoDesk Inventor*®		
50	Documentation drafting		
400	**Electric consumption in** kWh	**0.246 €**	**98.40 €**
1	**Annual *MATLAB*® license**	**800 €**	**800.00€**
1	**Annual *Microsoft Excel*® license**	**160 €**	**160.00 €**
1	**Annual *AutoDesk Inventor*® license.**	**1,985€**	**1,985.00€**
	Total cost (without Value Added Tax)		9,343.40 €
	VAT (21 %)		1,962.11 €
	Total estimated budget		**11,305.51€**

Table A.1: Estimated budget for the developed End of Degree project.

The estimated budget for the complete End of Degree project above developed is therefore ELEVEN THOUSAND THREE HUNDRED AND FIVE EUROS WITH FIFTY-ONE CENTS (11,305.51 €).

Appendix B

Scope statement

Given this project falls under the category of a technical initiative, the scope statement of the described product is included during this *Appendix*. Note that, however, given the academic nature of the initiative and the fact that it is by all means in the early stages of development, the conditions and requirements described will only refer to the general aspects necessarily covered during the model progress.

Firstly, the project deliverable is in the case a fully operational light helicopter model for private use, powered by a hydrogen fuel cell. Under the European Union norm, the aircraft must have the complete documentation in order, including its Initial Airworthiness Certificate (under Comission Regulation 748/2012 of the European Union), demonstrating the aircraft is in fact capable of developing the certification specifications of its type. Additionally, if required, additional documentation regarding the operation and maintenance of the different elements of the aircraft must be readily available at the end of the production cycle.

In terms of major objectives to be achieved during the project's development, the following checkpoints will be established with the objective of, very broadly, defining the trajectory to be followed in order to complete the project.

1. Develop a preliminary 3D model of the aircraft.
2. Perform aerodynamic tests to check the desired behaviour.
3. Obtain a detailed definition of the interior distribution of elements of the vehicle.
4. Perform detailed simulations of the aircraft behaviour and dynamics.
5. Build a miniature model to perform physical tests.
6. Establish the complete element distribution of the aircraft, defining the complete documentation regarding individual components and their assembly process, as well as their expected maintenance operations.
7. Develop and proceed with a sensible production plan to optimize the human and material resources within a reasonable but productive delivery time.

8. Perform flight tests on the prototype and develop an operating manual considering the experiences.

9. Once the design is optimized and produced, apply for the type certificate of the aircraft to obtain its initial airworthiness.

Finally, in terms of the workplace safety and health conditions, regulated by Spanish Royal Decree 486/1997 and the Law 31/1995 of Occupational Hazards Prevention, several measures are to be taken into consideration in order to not only follow the corresponding regulation but also ensure the well-being of workers. In terms of office environment, one must ensure that correct luminosity, temperature and noise conditions are those required by the worker so that not his/her health nor performance are affected. Tidiness and teamwork behaviour on the workplace must be encouraged in order to optimize working conditions.

In the case of later development of the project, sufficiently wide facilities must be prepared in order to carry out the assembly and, if needed, maintenance (according to the European Union norm 1321/2014). These facilities must be sufficiently isolated from environmental contamination and follow the aforementioned health recommendations. As for the corresponding storage location, rules must be enforced to ensure appropriate organization of the materials, separating those out of service and protecting others with restricted access.

Physically, the workplace must have facilitated emergency routes to orderly exit the building in case of need, as well as the corresponding emergency kits. Additionally, workers must be aware and trained in the use of these exits and materials by following sufficiently frequent drills and spending formation time related to workplace safety.

Appendix C

Adapted light helicopter blueprint

In the following page, the three-view drawing of the adapted light helicopter is shown. Note that, to avoid redundancy, only the one-passenger model was included given the exterior dimensions are the same across all variants except for the size of the fuel tanks.

Finally, credits to Pablo Tejada [56] and Serhii Taranets [35] for developing the previous models over which the tanks were introduced.

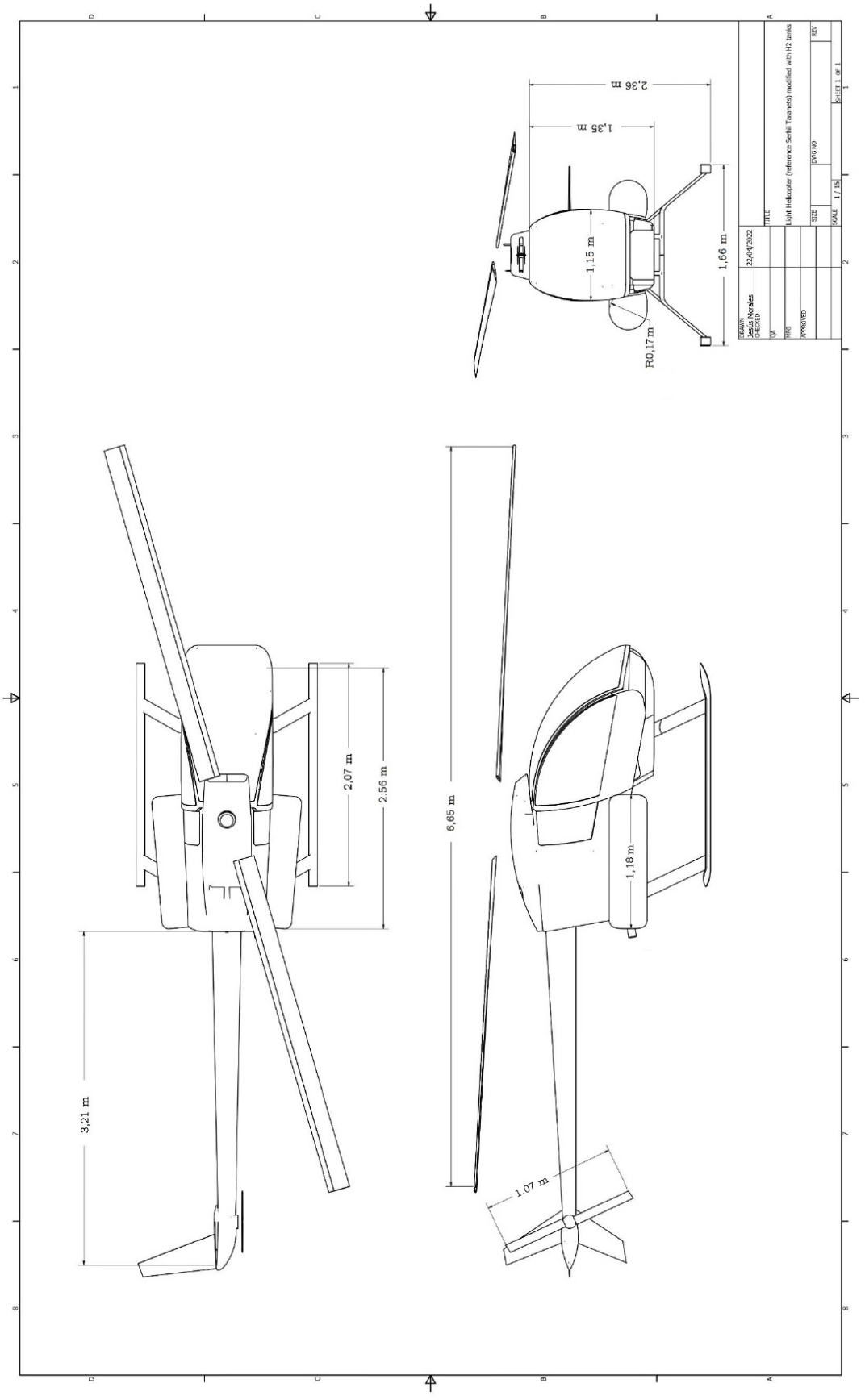
2,36 m
1,35 m
1,15 m
1,66 m
R0,17 m
DESIGN
Jesús Morales
CHECKED
QA
MFG
APPROVED
22/04/2022
TITLE
Light Helicopter (reference: Serfik Taranets) modified with H2 tanks
SIZE
DWG NO
REV
SCALE 1 / 15
SHEET 1 OF 1
2,07 m
2.56 m
3,21 m
6,65 m
1,18 m
1,07 m